

TIM LINDEN

PULSARS PRODUCE THE POSITRON EXCESS

2018 UCLA Dark Matter Meeting



THE OHIO STATE UNIVERSITY

CENTER FOR COSMOLOGY AND
ASTROPARTICLE PHYSICS

PULSARS PRODUCE THE POSITRON EXCESS

- ▶ **Always worry about the assumptions behind bold statements:**
 - ▶ **Observations necessitate these results.**
 - ▶ **Very few (and reasonable) modeling assumptions**

PULSARS PRODUCE THE POSITRON EXCESS

- ▶ **Radio and Gamma-Ray Data tell us that pulsars produce high-energy e^+e^- .**

- ▶ **What were the uncertainties in pulsar models?**

- ▶ **I: The e^+e^- production efficiency?**

Profumo (0812.4457); Malyshev et al. (0903.1310)

%.

A quantitative discussion of plausible values for f_{e^\pm} was recently given in Ref. [38]. We shall not review their discussion here, but Ref. [38] argues (see in particular their very informative App. B and C) that in the context of a standard model for the pulsar wind nebulae, a reasonable range for f_{e^\pm} falls between 1% and 30%.

- ▶ **II: The e^+e^- spectrum.**

- ▶ **III: The propagation of e^+e^- to Earth.**

PULSARS PRODUCE THE POSITRON EXCESS

- ▶ Radio and Gamma-Ray Data tell us that pulsars produce high-energy e^+e^- .

- ▶ What were the uncertainties in pulsar models?

- ▶ I: The e^+e^- production efficiency?

Profumo (0812.4457); Malyshev et al. (0903.1310)

%.

A quantitative discussion of plausible values for f_{e^\pm} was recently given in Ref. [38]. We shall not review their discussion here, but Ref. [38] argues (see in particular their very informative App. B and C) that in the context of a standard model for the pulsar wind nebulae, a reasonable range for f_{e^\pm} falls between 1% and 30%.

- ▶ II: The e^+e^- spectrum.

- ▶ III: The propagation of e^+e^- to Earth.

PULSARS PRODUCE THE POSITRON EXCESS

- ▶ Radio and Gamma-Ray Data tell us that pulsars produce high-energy e^+e^- .
- ▶ What were the uncertainties in pulsar models?
 - ▶ I: The e^+e^- production efficiency?
 - ▶ II: The e^+e^- spectrum.

Hooper et al. (0810.1527)

part of their energy adiabatically because of the expansion of the wind. The energy spectrum injected by a single pulsar depends on the environmental parameters of the pulsar, but some attempts to calculate the average spectrum injected by a population of mature pulsars suggest that the spectrum may be relatively hard, having a slope of $\sim 1.5-1.6$ [18]. This spectrum, however, results from a complex interplay of individual pulsar spectra, of the spatial and age distributions of pulsars in the Galaxy, and on the assumption that the chief channel for pulsar spin down is magnetic dipole radiation. Due to the related uncertainties, variations from this injection spectra cannot be ruled out. Typically, one concentrates the attention on pulsars of age $\sim 10^5$ years because younger pulsars are likely to still

- ▶ III: The propagation of e^+e^- to Earth.

PULSARS PRODUCE THE POSITRON EXCESS

- ▶ Radio and Gamma-Ray Data tell us that pulsars produce high-energy e^+e^- .
- ▶ What were the uncertainties in pulsar models?
 - ▶ I: The e^+e^- production efficiency?
 - ▶ II: The e^+e^- spectrum.
 - ▶ III: The propagation of e^+e^- to Earth. Malyshev et al. (0903.1310)

The observed spectrum on Earth of electrons and positrons injected by pulsars is also strongly dependent on propagation effects. In particular, the observed cutoff in the flux of electrons from a pulsar can be much smaller than the injection cutoff due to energy losses (“cooling”) during propagation. We define the cooling break, $E_{\text{br}}(t)$, as the maximal energy electrons can have after propagating for time t . Since – as stated above – the typical

TeV PULSAR OBSERVATIONS

Over the last year:

TeV gamma-ray observations have solved (or greatly reduced) these uncertainties.

The best-fit values support the pulsar interpretation.

TeV PULSAR OBSERVATIONS

Start without a theoretical model.

What do TeV observations tell us about pulsars?

THE E+E- PRODUCTION EFFICIENCY OF PULSARS

- ▶ **What were the uncertainties in pulsar models?**

- ▶ **I: The e⁺e⁻ production efficiency?**

Profumo (0812.4457); Malyshev et al. (0903.1310)

%.

A quantitative discussion of plausible values for f_{e^\pm} was recently given in Ref. [38]. We shall not review their discussion here, but Ref. [38] argues (see in particular their very informative App. B and C) that in the context of a standard model for the pulsar wind nebulae, a reasonable range for f_{e^\pm} falls between 1% and 30%.

Look at the closest systems

Geminga, Monogem:

Profumo (0812.4457)

TABLE II: Data for a few selected nearby pulsars and SNR's. E_{out} is the energy output in e^\pm pairs in units of 10^{48} erg (for the ST model column we assumed $f_{e^\pm} = 3\%$). The energy output for the SNR Loop I and Cygnus Loop are not estimated within the ST model, but via estimates of the total SNR output. The f_{e^\pm} column indicates the e^\pm output fraction used to compute the fluxes shown in fig. 4 and 5 assuming the ST model.

Name	Distance [kpc]	Age [yr]	\dot{E} [ergs/s]	E_{out} [ST]	E_{out} [CCY]	E_{out} [HR]	E_{out} [ZC]	f_{e^\pm}	g
Geminga [J0633+1746]	0.16	3.42×10^5	3.2×10^{34}	0.360	0.344	0.013	0.053	0.005	0.70
Monogem [B0656+14]	0.29	1.11×10^5	3.8×10^{34}	0.044	0.133	0.006	0.020	0.020	0.70
Vela [B0833-45]	0.29	1.13×10^4	6.9×10^{36}	0.084	0.456	0.006	0.372	0.0015	0.14
B0355+54	1.10	5.64×10^5	4.5×10^{34}	1.366	0.677	0.022	0.121	0.2	0.61
Loop I [SNR]	0.17	2×10^5		<i>0.3</i>				0.006	
Cygnus Loop [SNR]	0.44	2×10^4		<i>0.03</i>				0.01	

HAWC OBSERVATIONS OF GEMINGA AND MONOGEM

Name	Tested radius [°]	Index	$F_7 \times 10^{15}$ [$\text{TeV}^{-1} \text{cm}^{-2} \text{s}^{-1}$]	TeVCat
2HWC J0534+220	-	-2.58 ± 0.01	184.7 ± 2.4	Crab
2HWC J0631+169	-	-2.57 ± 0.15	6.7 ± 1.5	Geminga
"	2.0	-2.23 ± 0.08	48.7 ± 6.9	Geminga
2HWC J0635+180	-	-2.56 ± 0.16	6.5 ± 1.5	Geminga
2HWC J0700+143	1.0	-2.17 ± 0.16	13.8 ± 4.2	-
"	2.0	-2.03 ± 0.14	23.0 ± 7.3	-

▶ HAWC observes Geminga

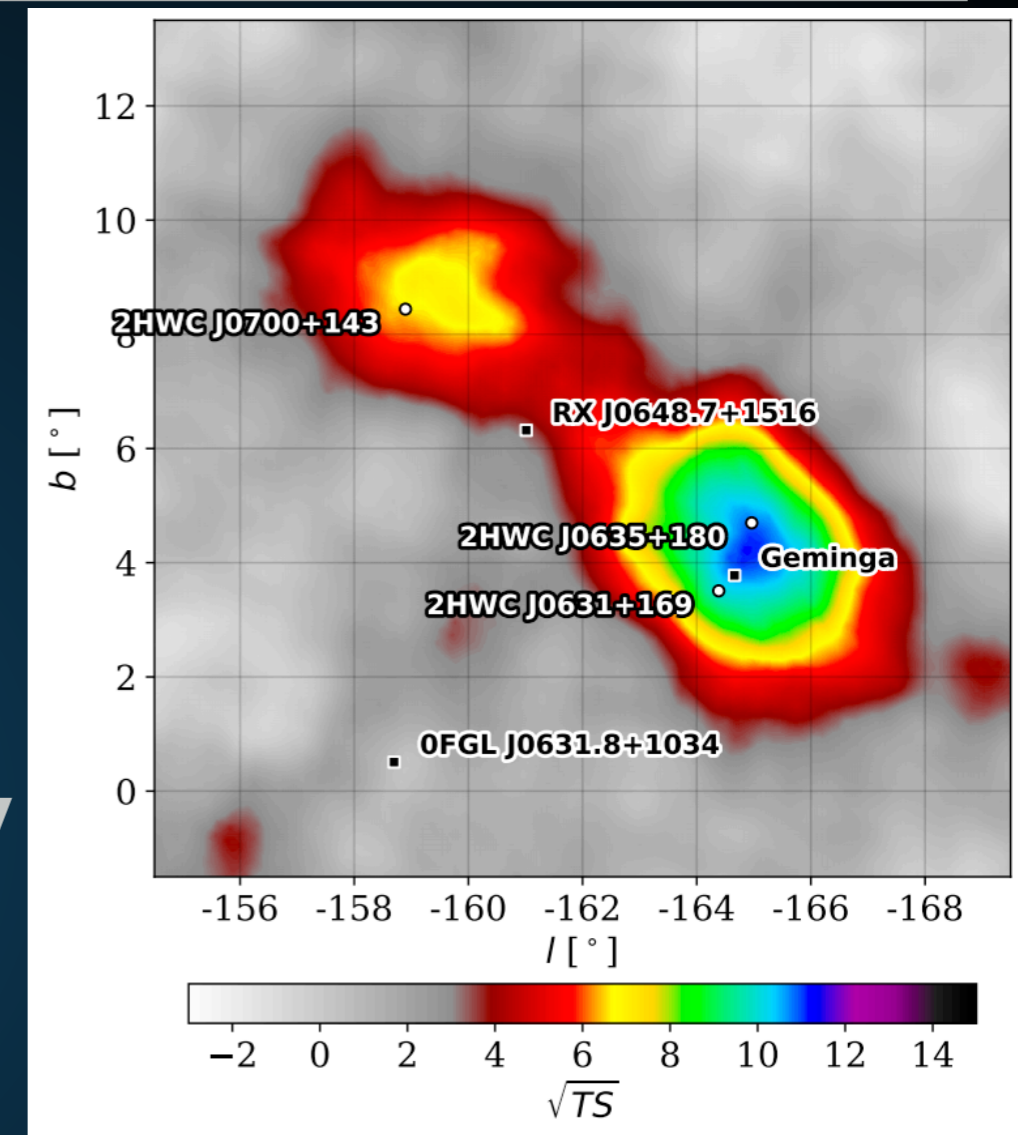
▶ $4.9 \times 10^{-14} \text{ TeV}^{-1} \text{ cm}^{-2} \text{ s}^{-1}$ at 7 TeV

▶ Luminosity $\sim 1.4 \times 10^{31} \text{ TeV s}^{-1}$

▶ Hard spectrum (-2.23)

▶ Moderate distance uncertainties.

We call these sources TeV halos



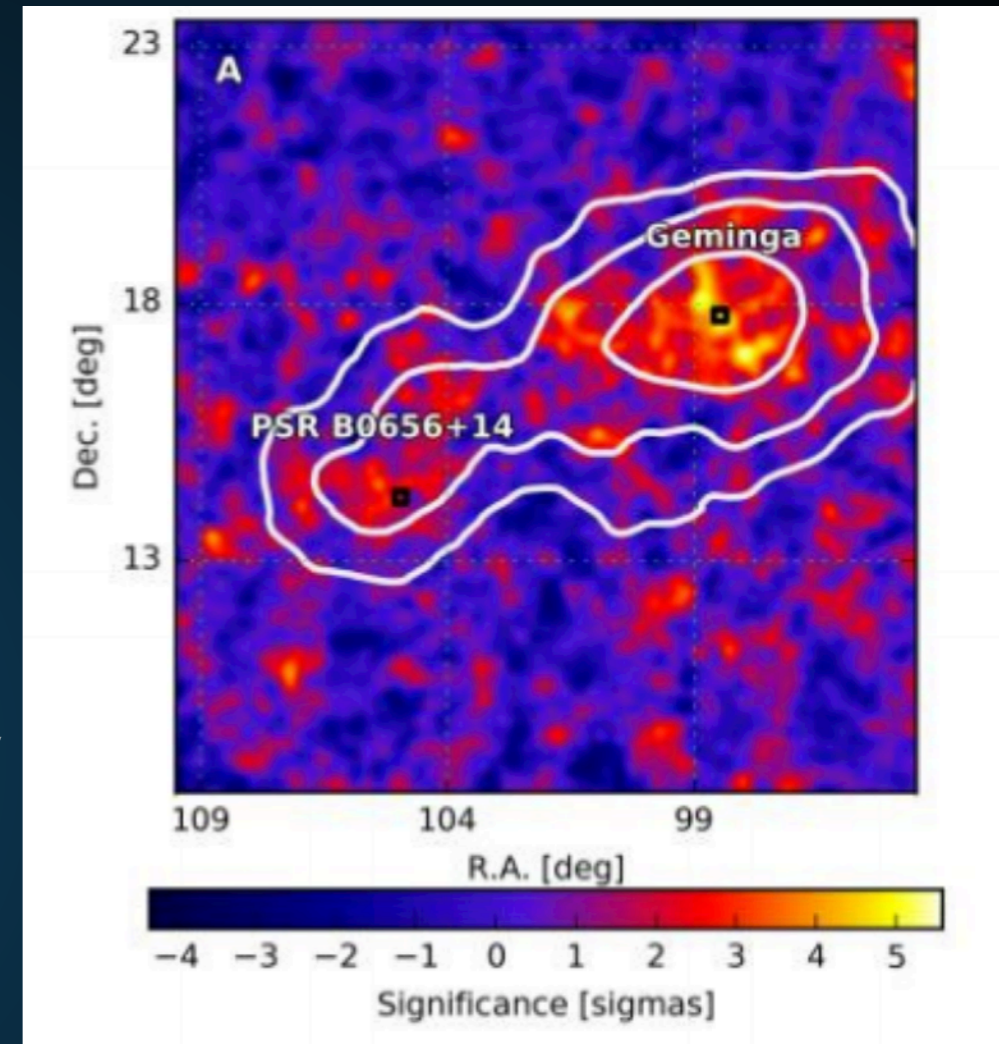
Beautiful !

HAWC OBSERVATIONS OF GEMINGA AND MONOGEM

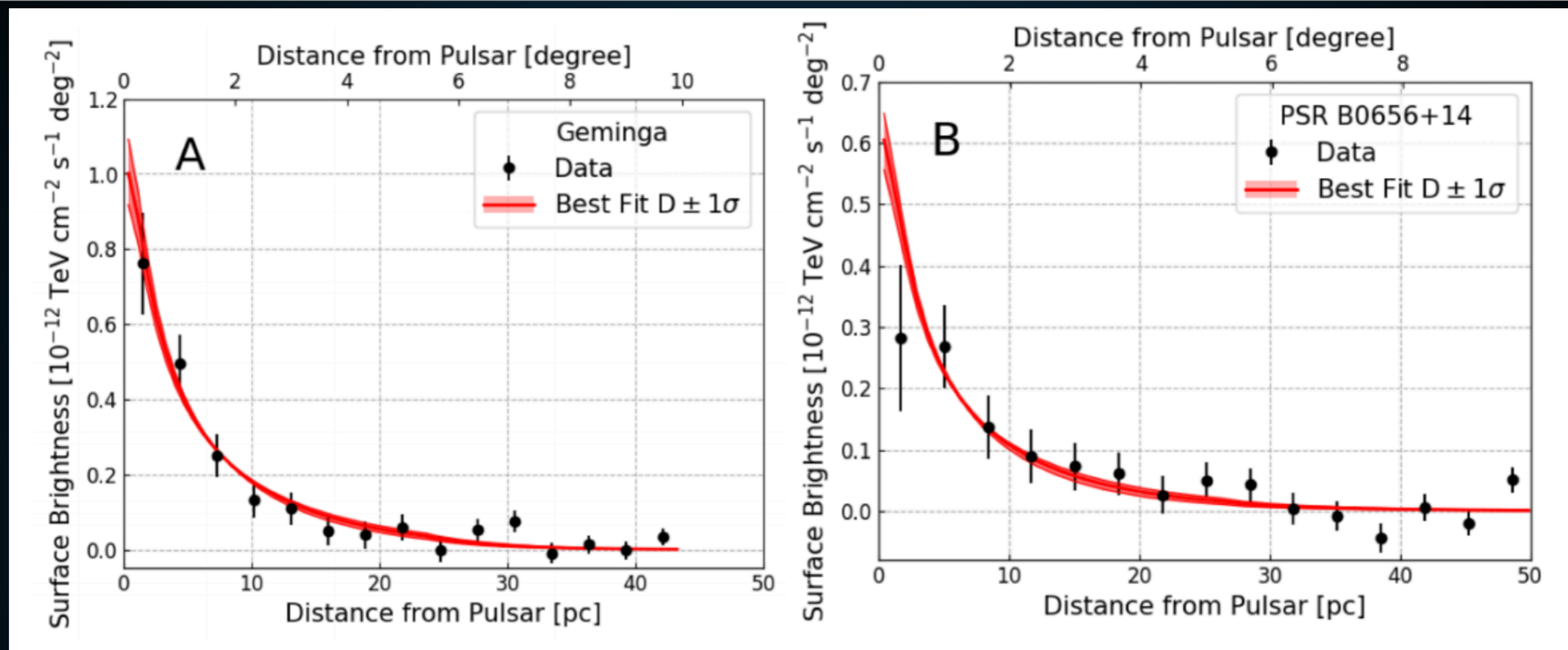
Name	Tested radius [$^{\circ}$]	Index	$F_7 \times 10^{15}$ [$\text{TeV}^{-1} \text{cm}^{-2} \text{s}^{-1}$]	TeVCat
2HWC J0700+143	1.0	-2.17 ± 0.16	13.8 ± 4.2	-
"	2.0	-2.03 ± 0.14	23.0 ± 7.3	-

- ▶ HAWC observes Monogem
 - ▶ $2.3 \times 10^{-14} \text{ TeV}^{-1} \text{ cm}^{-2} \text{ s}^{-1}$ at 7 TeV
 - ▶ Luminosity $\sim 1.1 \times 10^{31} \text{ TeV s}^{-1}$
 - ▶ Hard spectrum (-2.17)
 - ▶ Small distance uncertainties

We call these sources TeV halos



TEV HALOS



▶ Why Halos?

▶ These sources are extremely diffuse

▶ Evidence for electron acceleration and propagation far from the pulsar itself.

Combining the TeV luminosity and spectrum:

$\sim 3-9 \times 10^{33} \text{ erg s}^{-1} !$

9-27% of the total pulsar spin-down power!

▶ What were the uncertainties in pulsar models?

▶ I: The e^+e^- production efficiency?

Profumo (0812.4457); Malyshev et al. (0903.1310)

% . A quantitative discussion of plausible values for f_{e^\pm} was recently given in Ref. [38]. We shall not review their discussion here, but Ref. [38] argues (see in particular their very informative App. B and C) that in the context of a standard model for the pulsar wind nebulae, a reasonable range for f_{e^\pm} falls between 1% and 30%.

▶ II: The e^+e^- spectrum.

▶ III: The propagation of e^+e^- to Earth.

THE GLOBAL POPULATION OF TEV HALOS

- ▶ **Need to assume that other pulsars have a similar conversion efficiency**
- ▶ **TeV halos provide an observable way to test this!**

$$\phi_{\text{TeV halo}} = \left(\frac{\dot{E}_{\text{psr}}}{\dot{E}_{\text{Geminga}}} \right) \left(\frac{d_{\text{Geminga}}^2}{d_{\text{psr}}^2} \right) \phi_{\text{Geminga}}$$

- ▶ **Note: Using Monogem would increase fluxes by nearly a factor of 2. The power law of this correlation doesn't greatly affect the results.**

THE GLOBAL POPULATION OF TEV HALOS

► Many TeV halos observed by HESS with consistent fluxes

Table 1 HGPS sources considered as firmly identified pulsar wind nebulae in this paper.

HGPS name	ATNF name	Canonical name	$\lg \dot{E}$	τ_c (kyr)	d (kpc)	PSR offset (pc)	Γ	R_{PWN} (pc)	$L_{1-10 \text{ TeV}}$ ($10^{33} \text{ erg s}^{-1}$)
J1813-178 ^[1]	J1813-1749		37.75	5.60	4.70	< 2	2.07 ± 0.05	4.0 ± 0.3	19.0 ± 1.5
J1833-105	J1833-1034	G21.5-0.9 ^[2]	37.53	4.85	4.10	< 2	2.42 ± 0.19	< 4	2.6 ± 0.5
J1514-591	B1509-58	MSH 15-52 ^[3]	37.23	1.56	4.40	< 4	2.26 ± 0.03	11.1 ± 2.0	52.1 ± 1.8
J1930+188	J1930+1852	G54.1+0.3 ^[4]	37.08	2.89	7.00	< 10	2.6 ± 0.3	< 9	5.5 ± 1.8
J1420-607	J1420-6048	Kookaburra (K2) ^[5]	37.00	13.0	5.61	5.1 ± 1.2	2.20 ± 0.05	7.9 ± 0.6	44 ± 3
J1849-000	J1849-0001	IGR J18490-0000 ^[6]	36.99	42.9	7.00	< 10	1.97 ± 0.09	11.0 ± 1.9	12 ± 2
J1846-029	J1846-0258	Kes 75 ^[2]	36.91	0.728	5.80	< 2	2.41 ± 0.09	< 3	6.0 ± 0.7
J0835-455	B0833-45	Vela X ^[7]	36.84	11.3	0.280	2.37 ± 0.18	1.89 ± 0.03	2.9 ± 0.3	$0.83 \pm 0.11^*$
J1837-069 ^[8]	J1838-0655		36.74	22.7	6.60	17 ± 3	2.54 ± 0.04	41 ± 4	204 ± 8
J1418-609	J1418-6058	Kookaburra (Rabbit) ^[5]	36.69	10.3	5.00	7.3 ± 1.5	2.26 ± 0.05	9.4 ± 0.9	31 ± 3
J1356-645 ^[9]	J1357-6429		36.49	7.31	2.50	5.5 ± 1.4	2.20 ± 0.08	10.1 ± 0.9	14.7 ± 1.4
J1825-137 ^[10]	B1823-13		36.45	21.4	3.93	33 ± 6	2.38 ± 0.03	32 ± 2	116 ± 4
J1119-614	J1119-6127	G292.2-0.5 ^[11]	36.36	1.61	8.40	< 11	2.64 ± 0.12	14 ± 2	23 ± 4
J1303-631 ^[12]	J1301-6305		36.23	11.0	6.65	20.5 ± 1.8	2.33 ± 0.02	20.6 ± 1.7	96 ± 5

Table 4 Candidate pulsar wind nebulae from the pre-selection.

HGPS name	ATNF name	$\lg \dot{E}$	τ_c (kyr)	d (kpc)	PSR offset (pc)	Γ	R_{PWN} (pc)	$L_{1-10 \text{ TeV}}$ ($10^{33} \text{ erg s}^{-1}$)	Rating			
									1	2	3	4
J1616-508 (1)	J1617-5055	37.20	8.13	6.82	< 26	2.34 ± 0.06	28 ± 4	162 ± 9	★	★	★	★
J1023-575	J1023-5746	37.04	4.60	8.00	< 9	2.36 ± 0.05	23.2 ± 1.2	67 ± 5	★	★	★	★
J1809-193 (1)	J1811-1925	36.81	23.3	5.00	29 ± 7	2.38 ± 0.07	35 ± 4	53 ± 3	★	★	★	↓
J1857+026	J1856+0245	36.66	20.6	9.01	21 ± 6	2.57 ± 0.06	41 ± 9	118 ± 13	★	★	★	★
J1640-465	J1640-4631 (1)	36.64	3.35	12.8	< 20	2.55 ± 0.04	25 ± 8	210 ± 12	★	★	★	★
J1641-462	J1640-4631 (2)	36.64	3.35	12.8	50 ± 5	2.50 ± 0.11	< 14	17 ± 4	↓	*	★	*
J1708-443	B1706-44	36.53	17.5	2.60	17 ± 3	2.17 ± 0.08	12.7 ± 1.4	6.6 ± 0.9	★	★	★	★
J1908+063	J1907+0602	36.45	19.5	3.21	21 ± 3	2.26 ± 0.06	27.2 ± 1.5	28 ± 2	★	★	★	★
J1018-589A	J1016-5857 (1)	36.41	21.0	8.00	47.5 ± 1.6	2.24 ± 0.13	< 4	8.1 ± 1.4	↓	*	★	*
J1018-589B	J1016-5857 (2)	36.41	21.0	8.00	25 ± 7	2.20 ± 0.09	21 ± 4	23 ± 5	★	★	★	★
J1804-216	B1800-21	36.34	15.8	4.40	18 ± 5	2.69 ± 0.04	19 ± 3	42.5 ± 2.0	★	★	★	★
J1809-193 (2)	J1809-1917	36.26	51.3	3.55	< 17	2.38 ± 0.07	25 ± 3	26.9 ± 1.5	★	★	★	★
J1616-508 (2)	B1610-50	36.20	7.42	7.94	60 ± 7	2.34 ± 0.06	32 ± 5	220 ± 12	↓	★	★	★
J1718-385	J1718-3825	36.11	89.5	3.60	5.4 ± 1.6	1.77 ± 0.06	7.2 ± 0.9	4.6 ± 0.8	★	★	★	★
J1026-582	J1028-5819	35.92	90.0	2.33	9 ± 2	1.81 ± 0.10	5.3 ± 1.6	1.7 ± 0.5	↓	★	★	★
J1832-085	B1830-08 (1)	35.76	147	4.50	23.3 ± 1.5	2.38 ± 0.14	< 4	1.7 ± 0.4	↓	↓	★	*
J1834-087	B1830-08 (2)	35.76	147	4.50	32.3 ± 1.9	2.61 ± 0.07	17 ± 3	25.8 ± 2.0	↓	★	★	↓
J1858+020	J1857+0143	35.65	71.0	5.75	38 ± 3	2.39 ± 0.12	7.9 ± 1.6	7.1 ± 1.5	↓	★	★	↓
J1745-303	B1742-30 (1)	33.93	546	0.200	1.42 ± 0.15	2.57 ± 0.06	0.62 ± 0.07	0.014 ± 0.003	↓	↓	★	↓
J1746-308	B1742-30 (2)	33.93	546	0.200	< 1.1	3.3 ± 0.2	0.56 ± 0.12	0.009 ± 0.003	*	↓	★	↓

HAWC OBSERVATIONS OF TEV HALO LUMINOSITIES

ATNF Name	Dec. (°)	Distance (kpc)	Age (kyr)	Spindown Lum. (erg s ⁻¹)	Spindown Flux (erg s ⁻¹ kpc ⁻²)	2HWC
J0633+1746	17.77	0.25	342	3.2e34	4.1e34	2HWC J0631+169
B0656+14	14.23	0.29	111	3.8e34	3.6e34	2HWC J0700+143
B1951+32	32.87	3.00	107	3.7e36	3.3e34	—
J1740+1000	10.00	1.23	114	2.3e35	1.2e34	—
J1913+1011	10.18	4.61	169	2.9e36	1.1e34	2HWC J1912+099
J1831-0952	-9.86	3.68	128	1.1e36	6.4e33	2HWC J1831-098
J2032+4127	41.45	1.70	181	1.7e35	4.7e33	2HWC J2031+415
B1822-09	-9.58	0.30	232	4.6e33	4.1e33	—
B1830-08	-8.45	4.50	147	5.8e35	2.3e33	—
J1913+0904	9.07	3.00	147	1.6e35	1.4e33	—
B0540+23	23.48	1.56	253	4.1e34	1.4e33	—

- ▶ Can produce a ranked list of the 57 ATNF pulsars in the HAWC field of view.
- ▶ 5 of the brightest 7 have been detected.
- ▶ No dimmer systems have been detected.

HAWC OBSERVATIONS OF TEV HALO LUMINOSITIES

ATNF Name	Dec. (°)	Distance (kpc)	Age (kyr)	Spindown Lum. (erg s^{-1})	Spindown Flux ($\text{erg s}^{-1} \text{kpc}^{-2}$)	2HWC
J0633+1746	17.77	0.25	342	3.2e34	4.1e34	2HWC J0631+169
B0656+14	14.23	0.29	111	3.8e34	3.6e34	2HWC J0700+143
B1951+32	32.87	3.00	107	3.7e36	3.3e34	—
J1740+1000	10.00	1.23	114	2.3e35	1.2e34	—
J1913+1011	10.18	4.61	169	2.9e36	1.1e34	2HWC J1912+099
J1831-0952	-9.86	3.68	128	1.1e36	6.4e33	2HWC J1831-098
J2032+4127	41.45	1.70	181	1.7e35	4.7e33	2HWC J2031+415
B1822-09	-9.58	0.30	232	4.6e33	4.1e33	—
B1830-08	-8.45	4.50	147	5.8e35	2.3e33	—
J1913+0904	9.07	3.00	147	1.6e35	1.4e33	—
B0540+23	23.48	1.56	253	4.1e34	1.4e33	2HWC J0543+233

HAWC detection of TeV emission near PSR B0540+23

ATel #10941; *Colas Riviere (University of Maryland), Henrike Fleischhack (Michigan Technological University), Andres Sandoval (Universidad Nacional Autonoma de Mexico) on behalf of the HAWC collaboration*

on 9 Nov 2017; 23:11 UT

Credential Certification: Colas Riviere (riviere@umd.edu)

Subjects: Gamma Ray, TeV, VHE, Pulsar

 Tweet  Recommend 5

The High Altitude Water Cherenkov ([HAWC](#)) collaboration reports the discovery of a new TeV gamma-ray source HAWC J0543+233. It was discovered in a search for extended sources of radius 0.5° in a dataset of 911 days (ranging from November 2014 to August 2017) with a test statistic value of 36 (6σ pre-trials), following the method presented in [Abeysekara et al. 2017, ApJ, 843, 40](#). The measured J2000.0 equatorial position is RA= 85.78° , Dec= 23.40° with a statistical uncertainty of 0.2° . HAWC J0543+233 was close to passing the selection criteria of the 2HWC catalog ([Abeysekara et al. 2017, ApJ, 843, 40](#), see [HAWC J0543+233 in 2HWC map](#)), which it now fulfills with the additional data.

HAWC J0543+233 is positionally coincident with the pulsar PSR B0540+23 (Edot = $4.1e+34 \text{ erg s}^{-1}$, dist = 1.56 kpc, age = 253 kyr). It is the third low Edot, middle-aged pulsar announced to be detected with a TeV halo, along with Geminga and B0656+14. It was predicted to be one of the next such detection by HAWC by [Linden et al., 2017, arXiv:1703.09704](#).

Using a simple source model consisting of a disk of radius 0.5° , the measured spectral index is -2.3 ± 0.2 and the differential flux at 7 TeV is $(7.9 \pm 2.3) \times 10^{-15} \text{ TeV}^{-1} \text{ cm}^{-2} \text{ s}^{-1}$. The errors are

TeV HALOS PROVE THAT THE e^+e^- PRODUCTION EFFICIENCY IS HIGH

- ▶ What were the uncertainties in pulsar models?

- ▶ I: The e^+e^- production efficiency?

Profumo (0812.4457); [Malyshev et al. \(0903.1310\)](#)

% . A quantitative discussion of plausible values for f_{e^\pm} was recently given in Ref. [38]. We shall not review their discussion here, but Ref. [38] argues (see in particular their very informative App. B and C) that in the context of a standard model for the pulsar wind nebulae, a reasonable range for f_{e^\pm} falls between 1% and 30%.

- ▶ II: The e^+e^- spectrum.

- ▶ III: The propagation of e^+e^- to Earth.

- ▶ TeV observations solve this uncertainty - and prefer high numbers consistent with pulsar interpretations.

THE e^+e^- INJECTION SPECTRUM OF PULSARS

▶ II: The e^+e^- spectrum.

Hooper et al. (0810.1527)

part of their energy adiabatically because of the expansion of the wind. The energy spectrum injected by a single pulsar depends on the environmental parameters of the pulsar, but some attempts to calculate the average spectrum injected by a population of mature pulsars suggest that the spectrum may be relatively hard, having a slope of $\sim 1.5-1.6$ [18]. This spectrum, however, results from a complex interplay of individual pulsar spectra, of the spatial and age distributions of pulsars in the Galaxy, and on the assumption that the chief channel for pulsar spin down is magnetic dipole radiation. Due to the related uncertainties, variations from this injection spectra cannot be ruled out. Typically, one concentrates the attention on pulsars of age $\sim 10^5$ years because younger pulsars are likely to still

TeV HALO SPECTRUM

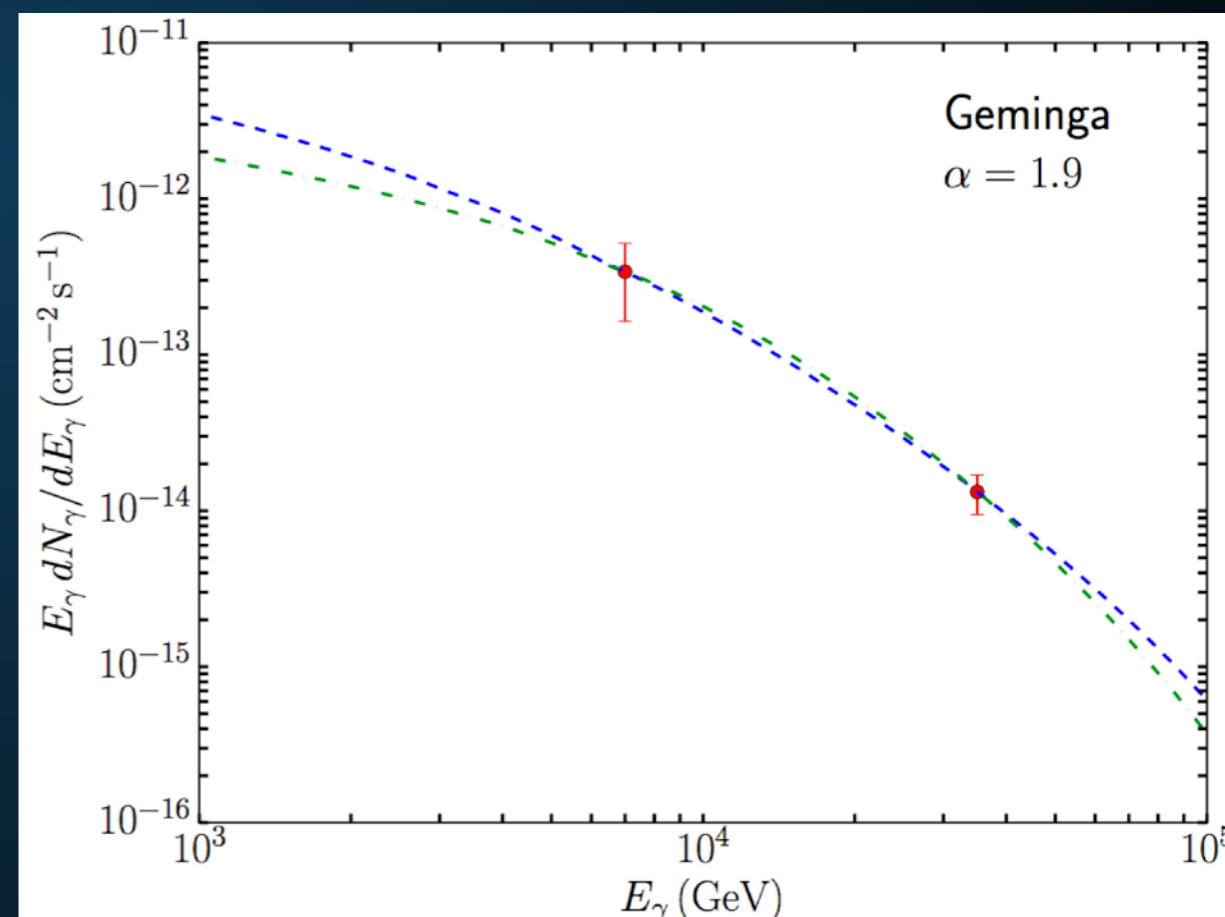
▶ Geminga has a hard gamma-ray spectrum

Name	Tested radius [$^{\circ}$]	Index	$F_7 \times 10^{15}$ [$\text{TeV}^{-1} \text{cm}^{-2} \text{s}^{-1}$]	TeVCat
2HWC J0631+169	-	-2.57 ± 0.15	6.7 ± 1.5	Geminga
”	2.0	-2.23 ± 0.08	48.7 ± 6.9	Geminga
2HWC J0635+180	-	-2.56 ± 0.16	6.5 ± 1.5	Geminga

▶ Based on a joint fit to the HAWC and Milagro data, we calculate:

▶ $-1.9 < \alpha < -1.5$

▶ $E_{\text{cut}} \cong 50 \text{ TeV}$



TEV HALO SPECTRUM

► This is compatible with the population of HESS sources

Table 1 HGPS sources considered as firmly identified pulsar wind nebulae in this paper.

HGPS name	ATNF name	Canonical name	$\lg \dot{E}$	τ_c (kyr)	d (kpc)	PSR offset (pc)	Γ	R_{PWN} (pc)	$L_{1-10 \text{ TeV}}$ ($10^{33} \text{ erg s}^{-1}$)
J1813-178 ^[1]	J1813-1749		37.75	5.60	4.70	< 2	2.07 ± 0.05	4.0 ± 0.3	19.0 ± 1.5
J1833-105	J1833-1034	G21.5-0.9 ^[2]	37.53	4.85	4.10	< 2	2.42 ± 0.19	< 4	2.6 ± 0.5
J1514-591	B1509-58	MSH 15-52 ^[3]	37.23	1.56	4.40	< 4	2.26 ± 0.03	11.1 ± 2.0	52.1 ± 1.8
J1930+188	J1930+1852	G54.1+0.3 ^[4]	37.08	2.89	7.00	< 10	2.6 ± 0.3	< 9	5.5 ± 1.8
J1420-607	J1420-6048	Kookaburra (K2) ^[5]	37.00	13.0	5.61	5.1 ± 1.2	2.20 ± 0.05	7.9 ± 0.6	44 ± 3
J1849-000	J1849-0001	IGR J18490-0000 ^[6]	36.99	42.9	7.00	< 10	1.97 ± 0.09	11.0 ± 1.9	12 ± 2
J1846-029	J1846-0258	Kes 75 ^[2]	36.91	0.728	5.80	< 2	2.41 ± 0.09	< 3	6.0 ± 0.7
J0835-455	B0833-45	Vela X ^[7]	36.84	11.3	0.280	2.37 ± 0.18	1.89 ± 0.03	2.9 ± 0.3	$0.83 \pm 0.11^*$
J1837-069 ^[8]	J1838-0655		36.74	22.7	6.60	17 ± 3	2.54 ± 0.04	41 ± 4	204 ± 8
J1418-609	J1418-6058	Kookaburra (Rabbit) ^[5]	36.69	10.3	5.00	7.3 ± 1.5	2.26 ± 0.05	9.4 ± 0.9	31 ± 3
J1356-645 ^[9]	J1357-6429		36.49	7.31	2.50	5.5 ± 1.4	2.20 ± 0.08	10.1 ± 0.9	14.7 ± 1.4
J1825-137 ^[10]	B1823-13		36.45	21.4	3.93	33 ± 6	2.38 ± 0.03	32 ± 2	116 ± 4
J1119-614	J1119-6127	G292.2-0.5 ^[11]	36.36	1.61	8.40	< 11	2.64 ± 0.12	14 ± 2	23 ± 4
J1303-631 ^[12]	J1301-6305		36.23	11.0	6.65	20.5 ± 1.8	2.33 ± 0.02	20.6 ± 1.7	96 ± 5

Table 4 Candidate pulsar wind nebulae from the pre-selection.

HGPS name	ATNF name	$\lg \dot{E}$	τ_c (kyr)	d (kpc)	PSR offset (pc)	Γ	R_{PWN} (pc)	$L_{1-10 \text{ TeV}}$ ($10^{33} \text{ erg s}^{-1}$)	Rating			
									1	2	3	4
J1616-508 (1)	J1617-5055	37.20	8.13	6.82	< 26	2.34 ± 0.06	28 ± 4	162 ± 9	★	★	★	★
J1023-575	J1023-5746	37.04	4.60	8.00	< 9	2.36 ± 0.05	23.2 ± 1.2	67 ± 5	★	★	★	★
J1809-193 (1)	J1811-1925	36.81	23.3	5.00	29 ± 7	2.38 ± 0.07	35 ± 4	53 ± 3	★	★	★	↓
J1857+026	J1856+0245	36.66	20.6	9.01	21 ± 6	2.57 ± 0.06	41 ± 9	118 ± 13	★	★	★	★
J1640-465	J1640-4631 (1)	36.64	3.35	12.8	< 20	2.55 ± 0.04	25 ± 8	210 ± 12	★	★	★	★
J1641-462	J1640-4631 (2)	36.64	3.35	12.8	50 ± 5	2.50 ± 0.11	< 14	17 ± 4	↓	*	★	*
J1708-443	B1706-44	36.53	17.5	2.60	17 ± 3	2.17 ± 0.08	12.7 ± 1.4	6.6 ± 0.9	★	★	★	★
J1908+063	J1907+0602	36.45	19.5	3.21	21 ± 3	2.26 ± 0.06	27.2 ± 1.5	28 ± 2	★	★	★	★
J1018-589A	J1016-5857 (1)	36.41	21.0	8.00	47.5 ± 1.6	2.24 ± 0.13	< 4	8.1 ± 1.4	↓	*	★	*
J1018-589B	J1016-5857 (2)	36.41	21.0	8.00	25 ± 7	2.20 ± 0.09	21 ± 4	23 ± 5	★	★	★	★
J1804-216	B1800-21	36.34	15.8	4.40	18 ± 5	2.69 ± 0.04	19 ± 3	42.5 ± 2.0	★	★	★	★
J1809-193 (2)	J1809-1917	36.26	51.3	3.55	< 17	2.38 ± 0.07	25 ± 3	26.9 ± 1.5	★	★	★	★
J1616-508 (2)	B1610-50	36.20	7.42	7.94	60 ± 7	2.34 ± 0.06	32 ± 5	220 ± 12	↓	★	★	★
J1718-385	J1718-3825	36.11	89.5	3.60	5.4 ± 1.6	1.77 ± 0.06	7.2 ± 0.9	4.6 ± 0.8	★	★	★	★
J1026-582	J1028-5819	35.92	90.0	2.33	9 ± 2	1.81 ± 0.10	5.3 ± 1.6	1.7 ± 0.5	↓	★	★	★
J1832-085	B1830-08 (1)	35.76	147	4.50	23.3 ± 1.5	2.38 ± 0.14	< 4	1.7 ± 0.4	↓	↓	★	*
J1834-087	B1830-08 (2)	35.76	147	4.50	32.3 ± 1.9	2.61 ± 0.07	17 ± 3	25.8 ± 2.0	↓	★	★	↓
J1858+020	J1857+0143	35.65	71.0	5.75	38 ± 3	2.39 ± 0.12	7.9 ± 1.6	7.1 ± 1.5	↓	★	★	↓
J1745-303	B1742-30 (1)	33.93	546	0.200	1.42 ± 0.15	2.57 ± 0.06	0.62 ± 0.07	0.014 ± 0.003	↓	↓	★	↓
J1746-308	B1742-30 (2)	33.93	546	0.200	< 1.1	3.3 ± 0.2	0.56 ± 0.12	0.009 ± 0.003	*	↓	★	↓

TEV HALO SPECTRUM

- ▶ **HAWC sources a bit softer - but depends sensitively on exponential cutoff that is expected near this energy:**

Name	Tested radius [$^{\circ}$]	Index	$F_7 \times 10^{15}$ [$\text{TeV}^{-1}\text{cm}^{-2}\text{s}^{-1}$]	TeVCat
2HWC J0631+169	-	-2.57 ± 0.15	6.7 ± 1.5	Geminga
"	2.0	-2.23 ± 0.08	48.7 ± 6.9	Geminga
2HWC J0635+180	-	-2.56 ± 0.16	6.5 ± 1.5	Geminga
2HWC J1831-098	-	-2.80 ± 0.09	44.2 ± 4.7	HESS J1831-098
"	0.9	-2.64 ± 0.06	95.8 ± 8.0	HESS J1831-098
2HWC J1912+099	-	-2.93 ± 0.09	14.5 ± 1.9	HESS J1912+101
"	0.7	-2.64 ± 0.06	36.6 ± 3.0	HESS J1912+101
2HWC J0700+143	1.0	-2.17 ± 0.16	13.8 ± 4.2	-
"	2.0	-2.03 ± 0.14	23.0 ± 7.3	-
2HWC J2031+415	-	-2.57 ± 0.07	32.4 ± 3.2	TeV J2032+4130
"	0.7	-2.52 ± 0.05	61.6 ± 4.4	TeV J2032+4130

- ▶ **Softer spectra are preferred, due to observed softening in the e^+e^- spectrum by AMS-02.**

TeV HALO SPECTRUM

- ▶ TeV observations still have uncertainties, but have verified the general scenario where:
 - ▶ $-1.9 < \alpha < -1.5$
 - ▶ Some indication that most sources are on the softer end.

- ▶ What were the uncertainties in pulsar models?

- ▶ I: The e^+e^- production efficiency?

- ▶ II: The e^+e^- spectrum.

Hooper et al. (0810.1527)

part of their energy adiabatically because of the expansion of the wind. The energy spectrum injected by a single pulsar depends on the environmental parameters of the pulsar, but some attempts to calculate the average spectrum injected by a population of mature pulsars suggest that the spectrum may be relatively hard, having a slope of $\sim 1.5-1.6$ [18]. This spectrum, however, results from a complex interplay of individual pulsar spectra, of the spatial and age distributions of pulsars in the Galaxy, and on the assumption that the chief channel for pulsar spin down is magnetic dipole radiation. Due to the related uncertainties, variations from this injection spectra cannot be ruled out. Typically, one concentrates the attention on pulsars of age $\sim 10^5$ years because younger pulsars are likely to still

- ▶ III: The propagation of e^+e^- to Earth.

THE PROPAGATION OF e^+e^- TO EARTH

▶ III: The propagation of e^+e^- to Earth. Malyshev et al. (0903.1310)

The observed spectrum on Earth of electrons and positrons injected by pulsars is also strongly dependent on propagation effects. In particular, the observed cutoff in the flux of electrons from a pulsar can be much smaller than the injection cutoff due to energy losses (“cooling”) during propagation. We define the cooling break, $E_{\text{br}}(t)$, as the maximal energy electrons can have after propagating for time t . Since – as stated above – the typical

WHAT HAPPENS TO THE LOW-ENERGY E^+E^- ?

- ▶ So far: **1-10 TeV gamma-rays (3-30 TeV e^+e^-)**
- ▶ What happens at lower energies?
- ▶ Need a pinch of theory.

WHAT HAPPENS TO THE LOW-ENERGY E⁺E⁻?

$$\tau_{\text{diff}} \propto \frac{L^2}{D_0 E^\delta} \quad \tau_{\text{loss}} \propto E^{-1}$$

$$L(E) \propto \sqrt{D_0 E^{\delta-1}}$$

- ▶ In general, low-energy electrons travel farther before losing their energy.
- ▶ At ~30 TeV, the electrons traveled ~25 pc
- ▶ How far do the low-energy electrons go?

WHAT HAPPENS TO THE LOW-ENERGY e^+e^- ?

Back to Observations!

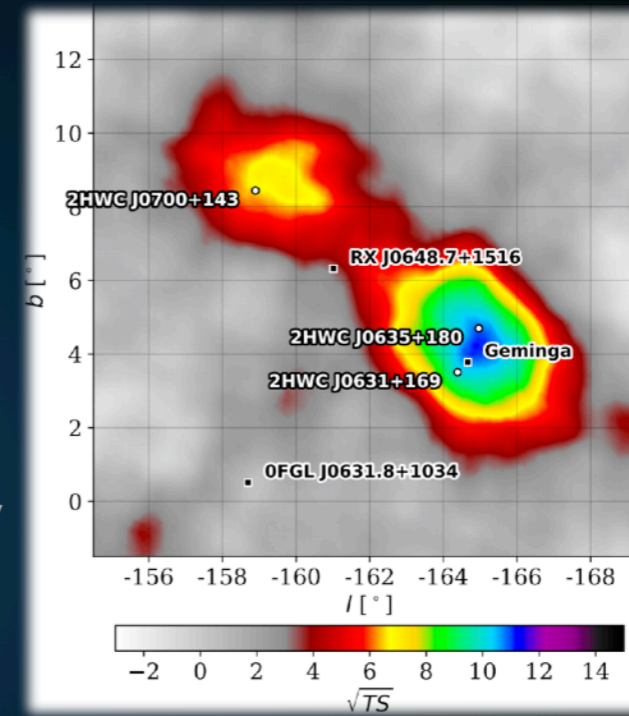
ELECTRON DIFFUSION WITHIN TEV HALOS

HAWC OBSERVATIONS OF GEMINGA AND MONOGEM

Name	Tested radius [$^{\circ}$]	Index	$F_7 \times 10^{15}$ [$\text{TeV}^{-1} \text{cm}^{-2} \text{s}^{-1}$]	TeVCat
2HWC J0534+220	-	-2.58 ± 0.01	184.7 ± 2.4	Crab
2HWC J0631+169	-	-2.57 ± 0.15	6.7 ± 1.5	Geminga
"	2.0	-2.23 ± 0.08	48.7 ± 6.9	Geminga
2HWC J0635+180	-	-2.56 ± 0.16	6.5 ± 1.5	Geminga
2HWC J0700+143	1.0	-2.17 ± 0.16	13.8 ± 4.2	-
"	2.0	-2.03 ± 0.14	23.0 ± 7.3	-

▶ HAWC observes Geminga

- ▶ $4.9 \times 10^{-14} \text{TeV}^{-1} \text{cm}^{-2} \text{s}^{-1}$ at 7 TeV
- ▶ Luminosity $\sim 1.4 \times 10^{31} \text{TeV s}^{-1}$
- ▶ Hard spectrum (-2.23)
- ▶ Moderate distance uncertainties.



Beautiful !

These sources are bright!

The high-energy electrons must be confined.

- ▶ The energy loss timescale in the ISM ($5 \mu\text{G}$; 1 eV cm^{-3}) is approximately:

$$\tau_{\text{loss}} \approx 2 \times 10^4 \text{ yr} \left(\frac{10 \text{ TeV}}{E_e} \right)$$

- ▶ For standard diffusion ($D_0 = 5 \times 10^{28} \text{ cm}^2\text{s}^{-1}$, $\delta=0.33$), this implies a radial extent of $\sim 250 \text{ pc}$.

- ▶ 20 pc extent indicates $D_0 \sim 1 \times 10^{26} \text{ cm}^2 \text{ s}^{-1}$

27 Feb 2017

HAWC Observations Strongly Favor Pulsar Interpretations of the Cosmic-Ray Positron Excess

Dan Hooper,^{a,b,c} Ilias Cholis,^d Tim Linden^e and Ke...

^aFermi National Accelerator Laboratory, Center for Particle Astrophysics

^bUniversity of Chicago, Department of Astronomy and Astrophysics

^cUniversity of Chicago, Kavli Institute for Cosmological Physics

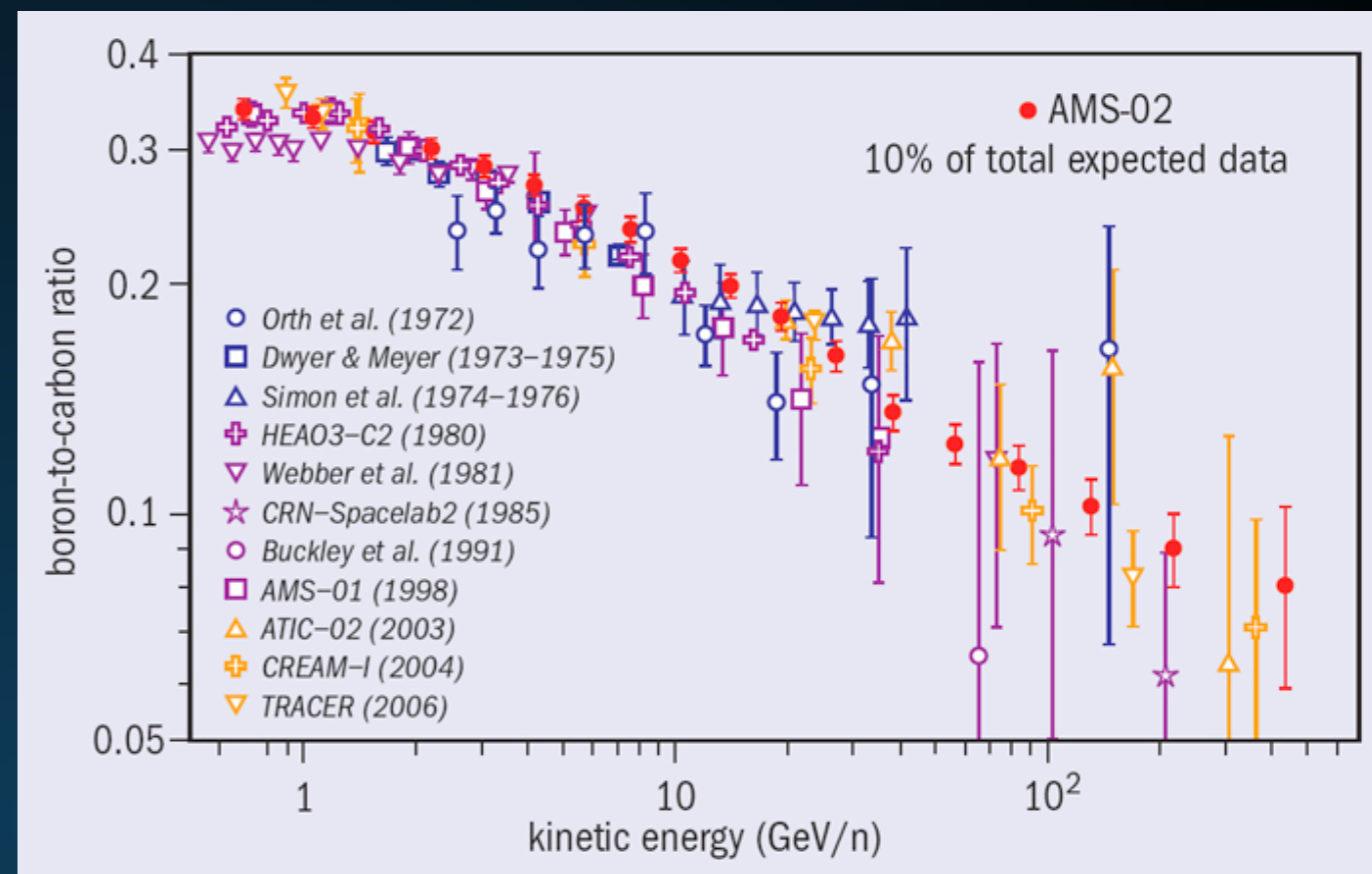
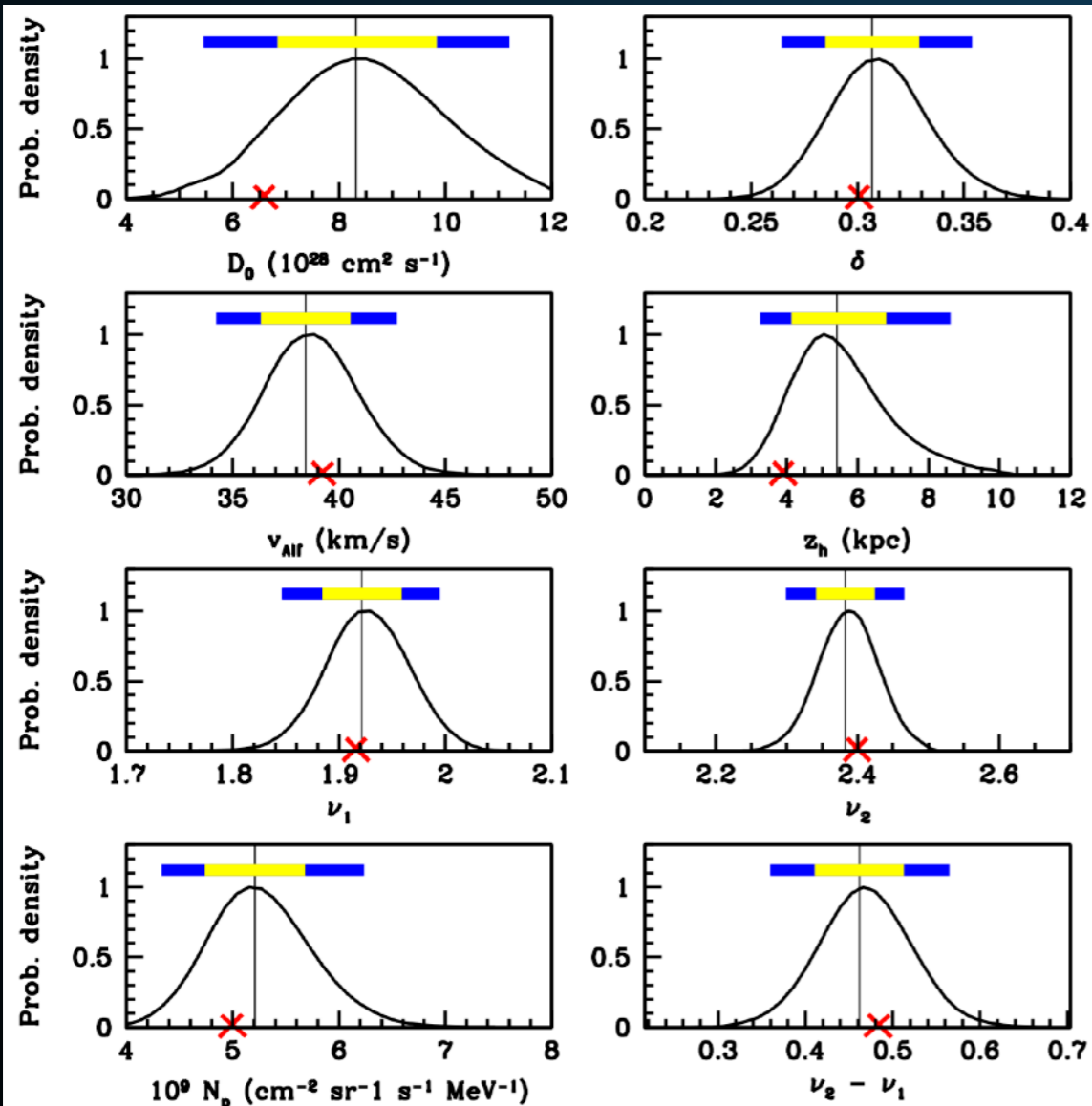
^dDepartment of Physics and Astronomy, The Johns Hopkins University, Center for Cosmology and AstroParticle Physics

^eDepartment of Astronomy, College Park, MD, 20725

jhu.edu, linden@jhu.edu

EFFECT OF TEV HALOS ON ISM PROPAGATION

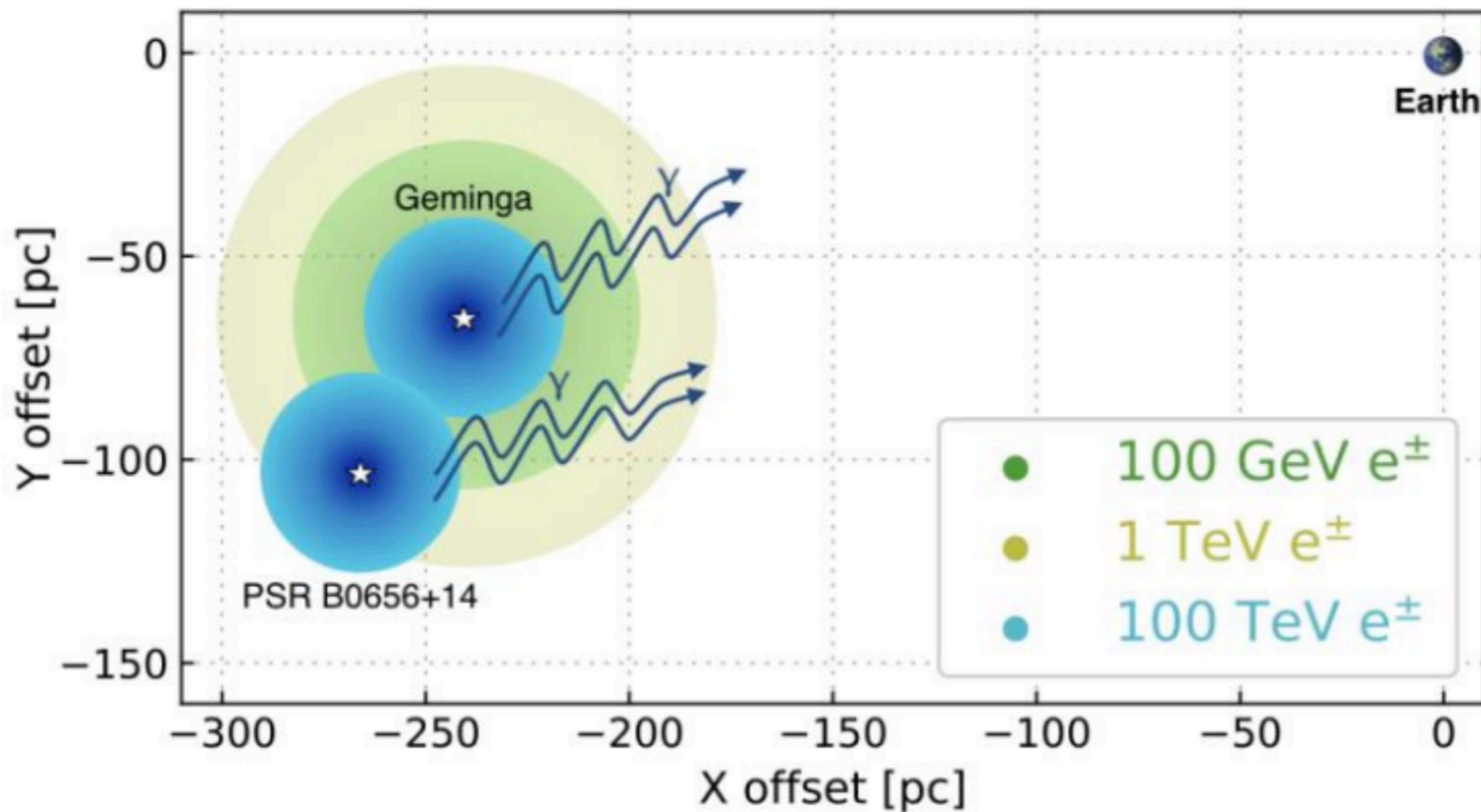
- ▶ **Multiple cosmic-ray observations indicate that the average diffusion constant is $\sim 5 \times 10^{28} \text{ cm}^2 \text{ s}^{-1}$**

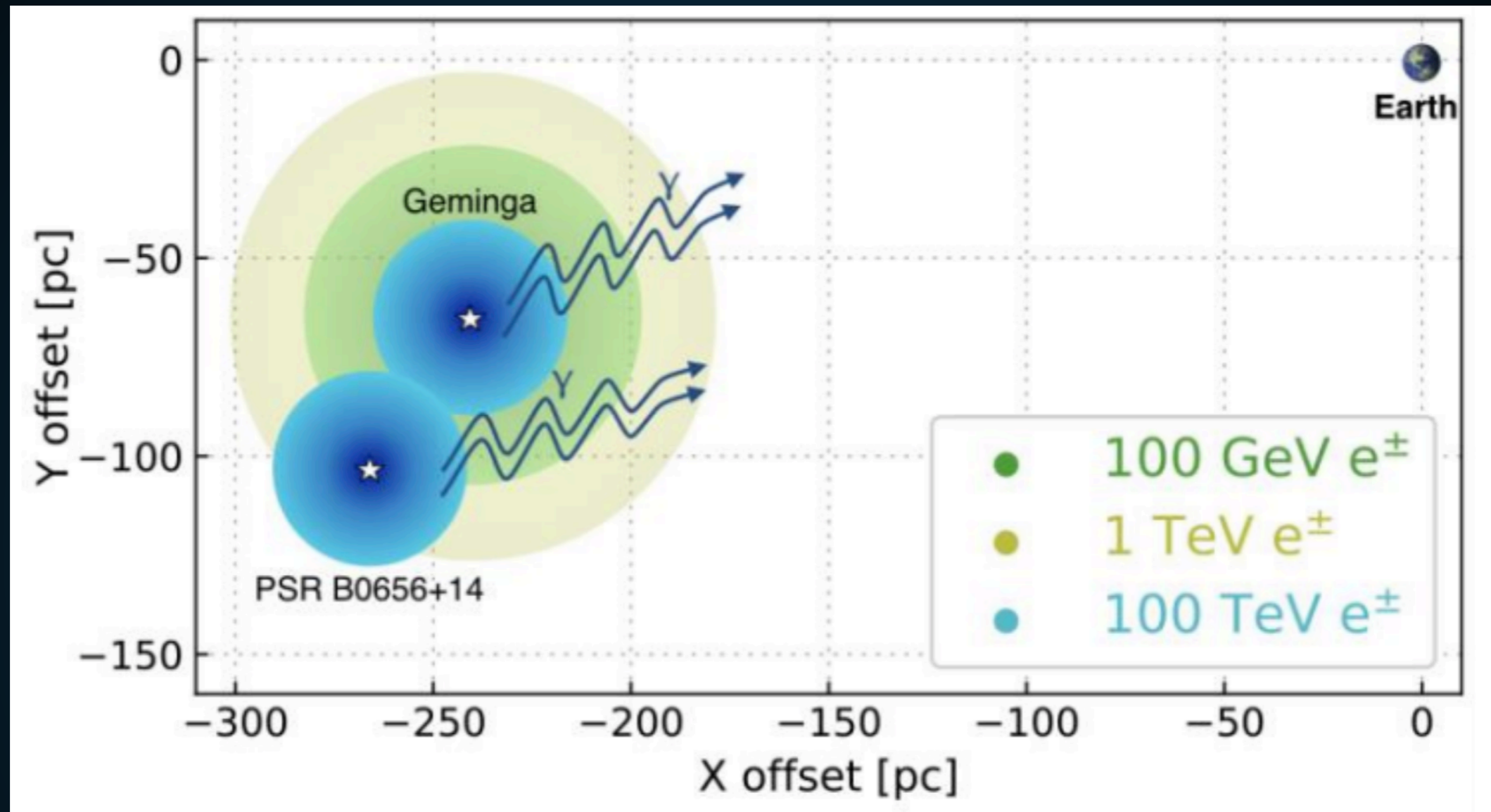


- ▶ **How do we reconcile these two observations?**

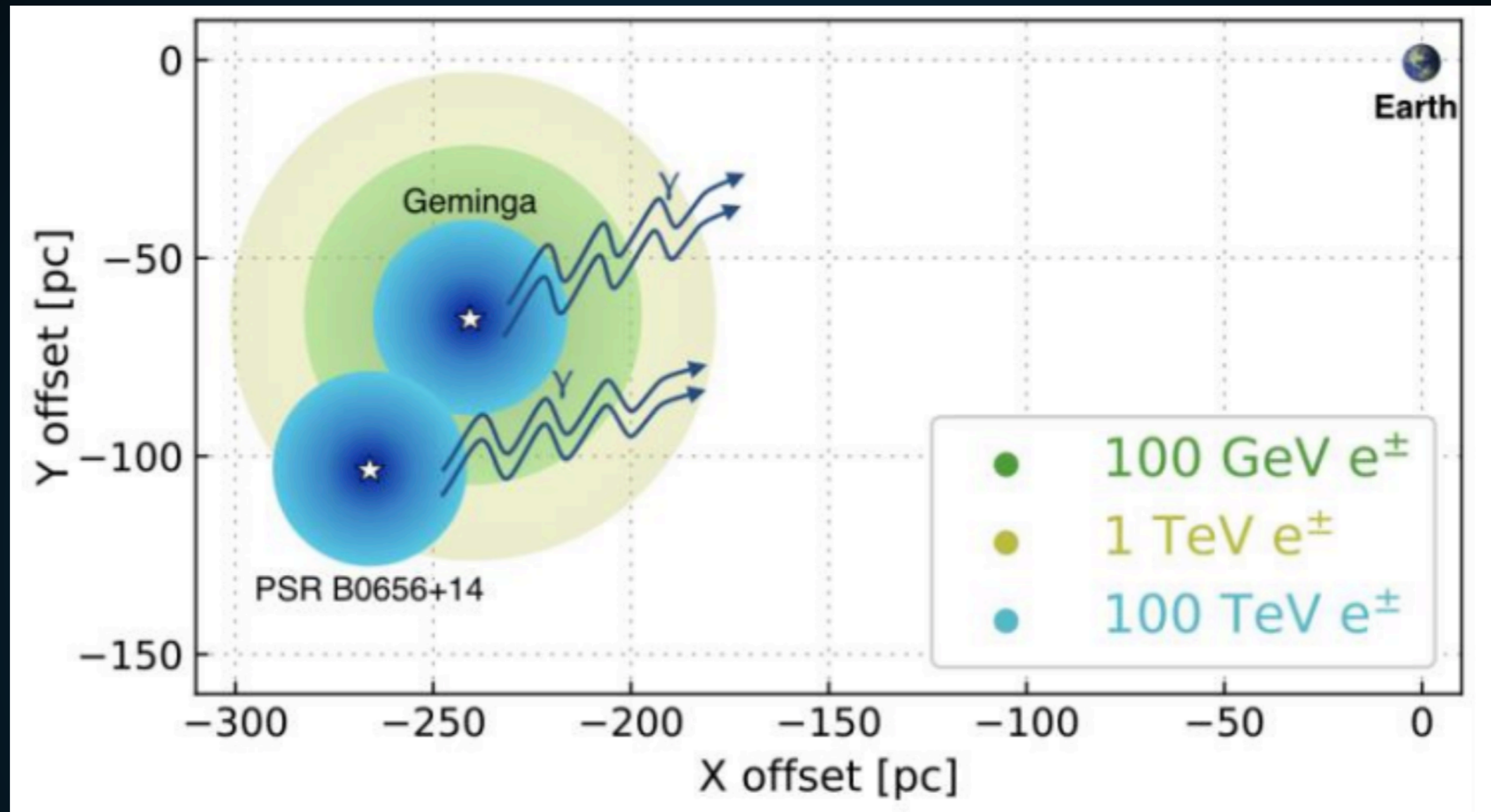
TWO PIECES OF INFORMATION

HAWC Collaboration (1711.06223)





- ▶ **Assumption 1:** The diffusion constant measured near Geminga and Monogem stands as the first measurement of the diffusion constant near Earth



- ▶ Methodology: Apply the low ($D_0 \sim 1 \times 10^{26} \text{ cm}^2 \text{ s}^{-1}$) diffusion constant for the full positron journey.

TWO POSSIBLE ASSUMPTIONS

$$\tau_{\text{diff}} \propto \frac{L^2}{D_0 E^\delta} \quad \tau_{\text{loss}} \propto E^{-1}$$

$$L(E) \propto \sqrt{D_0 E^{\delta-1}}$$

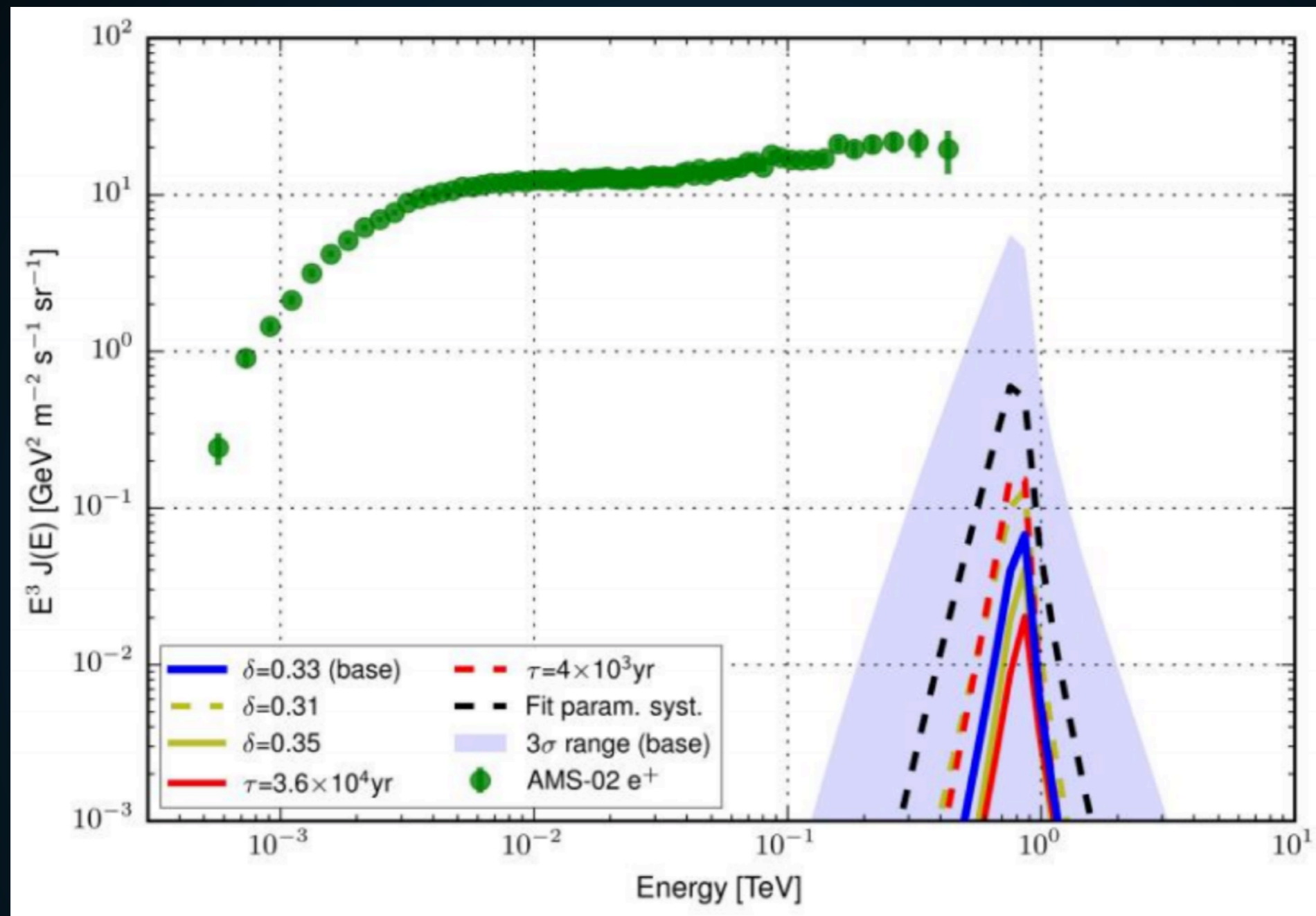
- ▶ **Implication: Assuming Kolmogorov Diffusion ($\delta = 0.33$), 100 GeV e^+e^- propagate about 4.5x as far.**

TWO POSSIBLE ASSUMPTIONS

$$L(10 \text{ TeV}) = 20 \text{ pc}$$

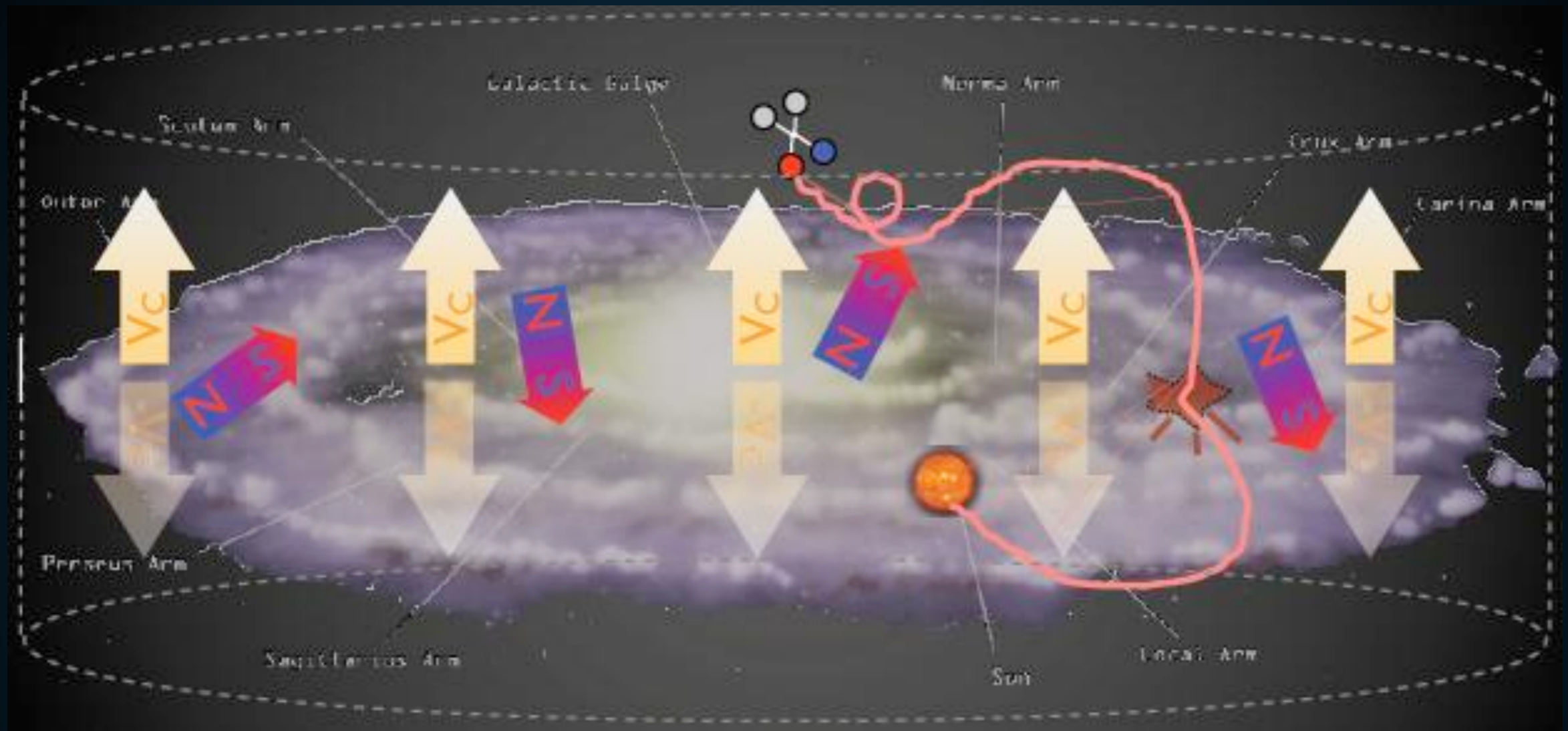
$$L(100 \text{ GeV}) = 92 \text{ pc}$$

- ▶ **Implication: Assuming Kolmogorov Diffusion ($\delta = 0.33$), 100 GeV electrons propagate about 4.5x as far.**
- ▶ **Earth is ~250 pc away**



- **Implication: Geminga and Monogem do not explain the positron excess.**

TWO POSSIBLE ASSUMPTIONS



- ▶ **Assumption 2: Measurements of cosmic-ray primary to secondary ratios (e.g. by AMS-02) imply that the local diffusion constant is high. The diffusion constant near Geminga and Monogem is local to those sources.**

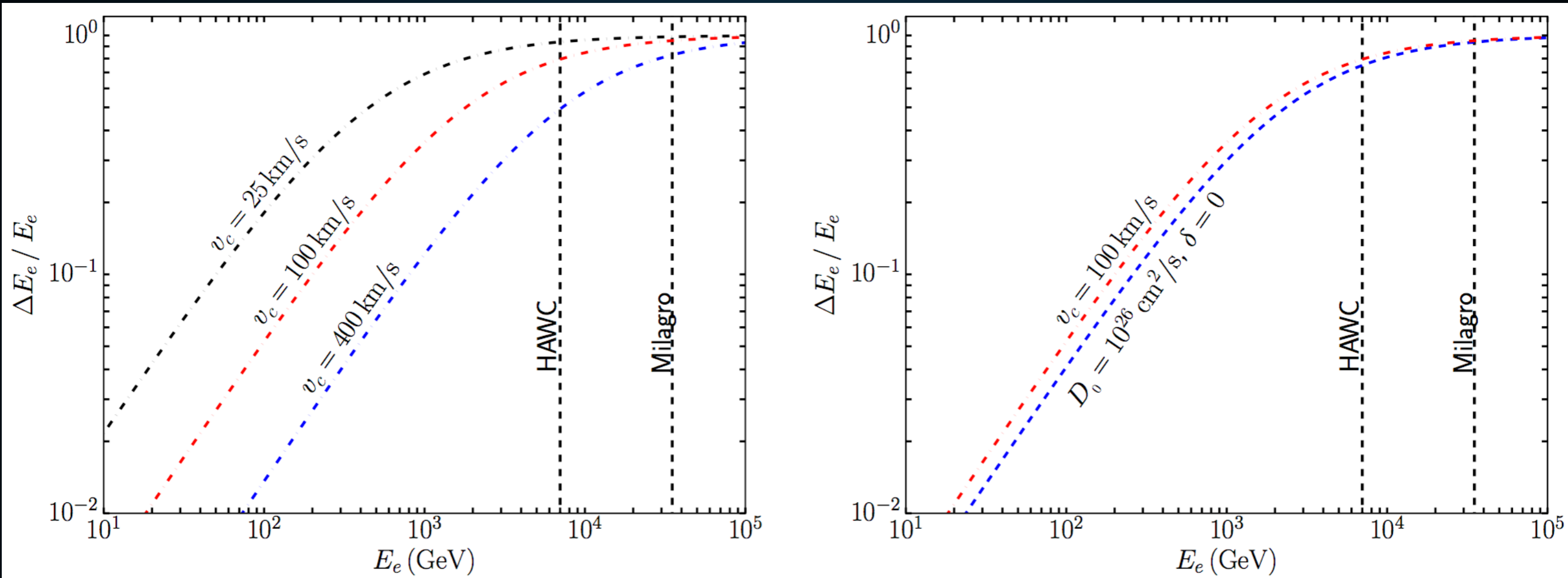
WHAT HAPPENS TO THE LOW-ENERGY E+E-?

Two Zone Model: First electrons escape from halo

$$\tau_{\text{diff}} \propto \frac{L^2}{D_0 E^\delta} \quad \tau_{\text{loss}} \propto E^{-1}$$
$$\left(\frac{\Delta E}{E} \right) \propto \frac{\tau_{\text{diff}}}{\tau_{\text{loss}}} \propto E^{1-\delta}$$

- ▶ Low-energy electrons lose energy slower, lose less energy before exiting the TeV halo.
- ▶ If 10 TeV electrons lose 90% of their energy, 100 GeV electrons lose 10% of their energy.

Two Zone Model: First electrons escape from halo



- ▶ **Low-energy electrons lose energy slower, lose less energy before exiting the TeV halo.**
- ▶ **If 10 TeV electrons lose 90% of their energy, 100 GeV electrons lose 10% of their energy.**

WHAT HAPPENS TO THE LOW-ENERGY E+E-?

Two Zone Model: Then electrons propagate through ISM

ELECTRON DIFFUSION NEAR TEV HALOS

1702.08436

- ▶ The energy loss timescale in the ISM ($5 \mu\text{G}$; 1 eV cm^{-3}) is approximately:

$$\tau_{\text{loss}} \approx 2 \times 10^4 \text{ yr} \left(\frac{10 \text{ TeV}}{E_e} \right)$$

- ▶ For ISM Diffusion ($D_0 = 5 \times 10^{28} \text{ cm}^2 \text{ s}^{-1}$, $\delta=0.33$), this implies a radial extent of $\sim 250 \text{ pc}$.

- ▶ 20 pc extent indicates $D_0 \sim 1 \times 10^{26} \text{ cm}^2 \text{ s}^{-1}$

27 Feb 2017

HAWC Observations Strongly Favor Pulsar Interpretations of the Cosmic-Ray Positron Excess

Dan Hooper,^{a,b,c} Ilias Cholis,^d Tim Linden^e and Ke F...

^aFermi National Accelerator Laboratory, Center for Particle Astrophysics
^bUniversity of Chicago, Department of Astronomy and Astrophysics
^cUniversity of Chicago, Kavli Institute for Cosmological Physics
^dDepartment of Physics and Astronomy, The Johns Hopkins University
^eDepartment of Astronomy and Astrophysics, University of Maryland, College Park, MD, 20742

ihp.edu, linden

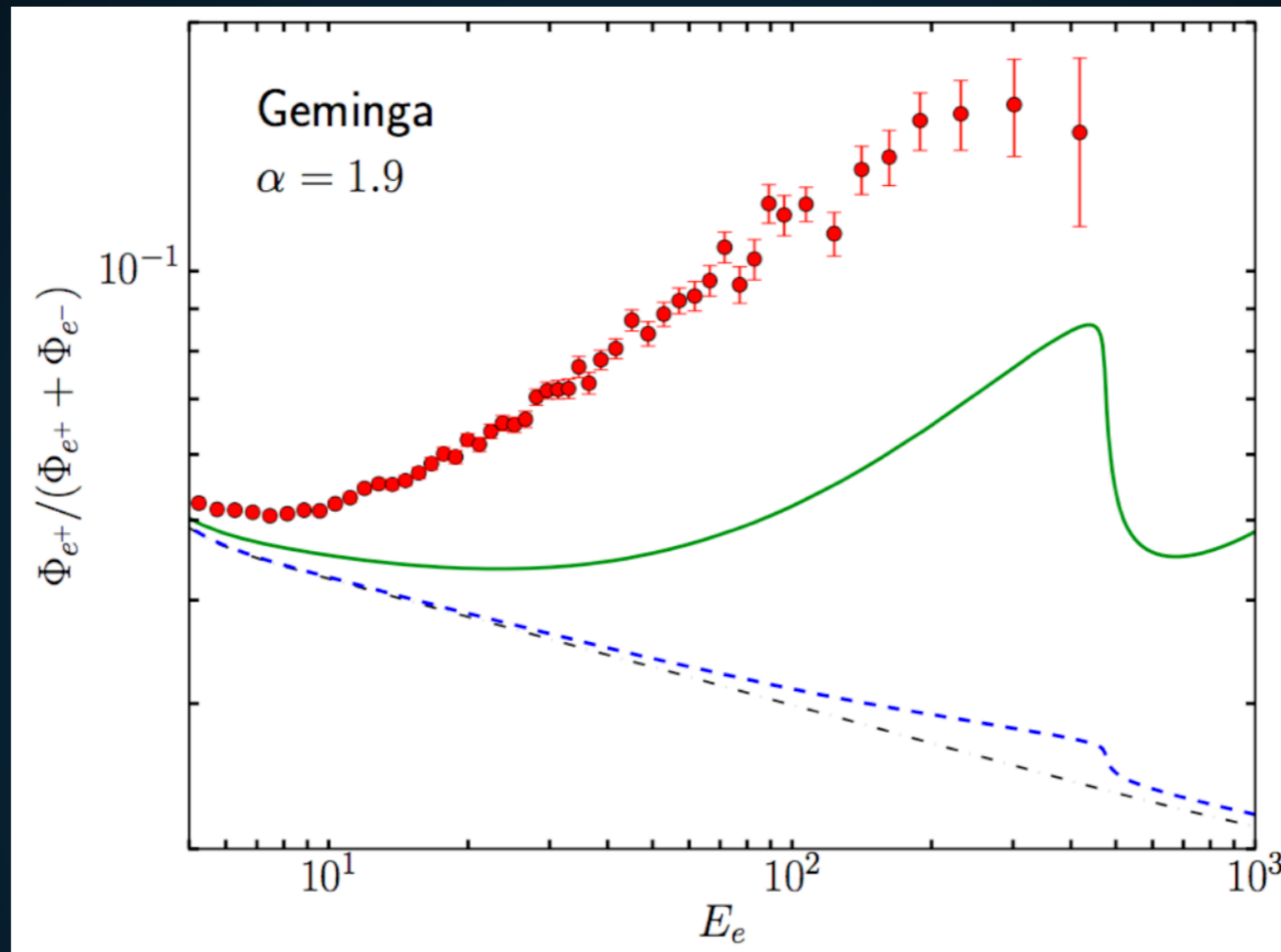
- ▶ Outside the TeV halo, diffusion is 500x more efficient.

WHAT HAPPENS TO THE LOW-ENERGY E^+E^- ?

Two Zone Model: Then electrons propagate through ISM

$$\tau_{\text{diff}} \propto \frac{L^2}{D_0 E^\delta} \quad \tau_{\text{loss}} \propto E^{-1}$$
$$L(E) \propto \sqrt{D_0 E^{\delta-1}}$$

- ▶ Instead of 100 GeV electrons propagating ~ 90 pc, they now propagate 2000 pc.



- **Implication: Low energy positrons make it to Earth and explain the positron excess.**

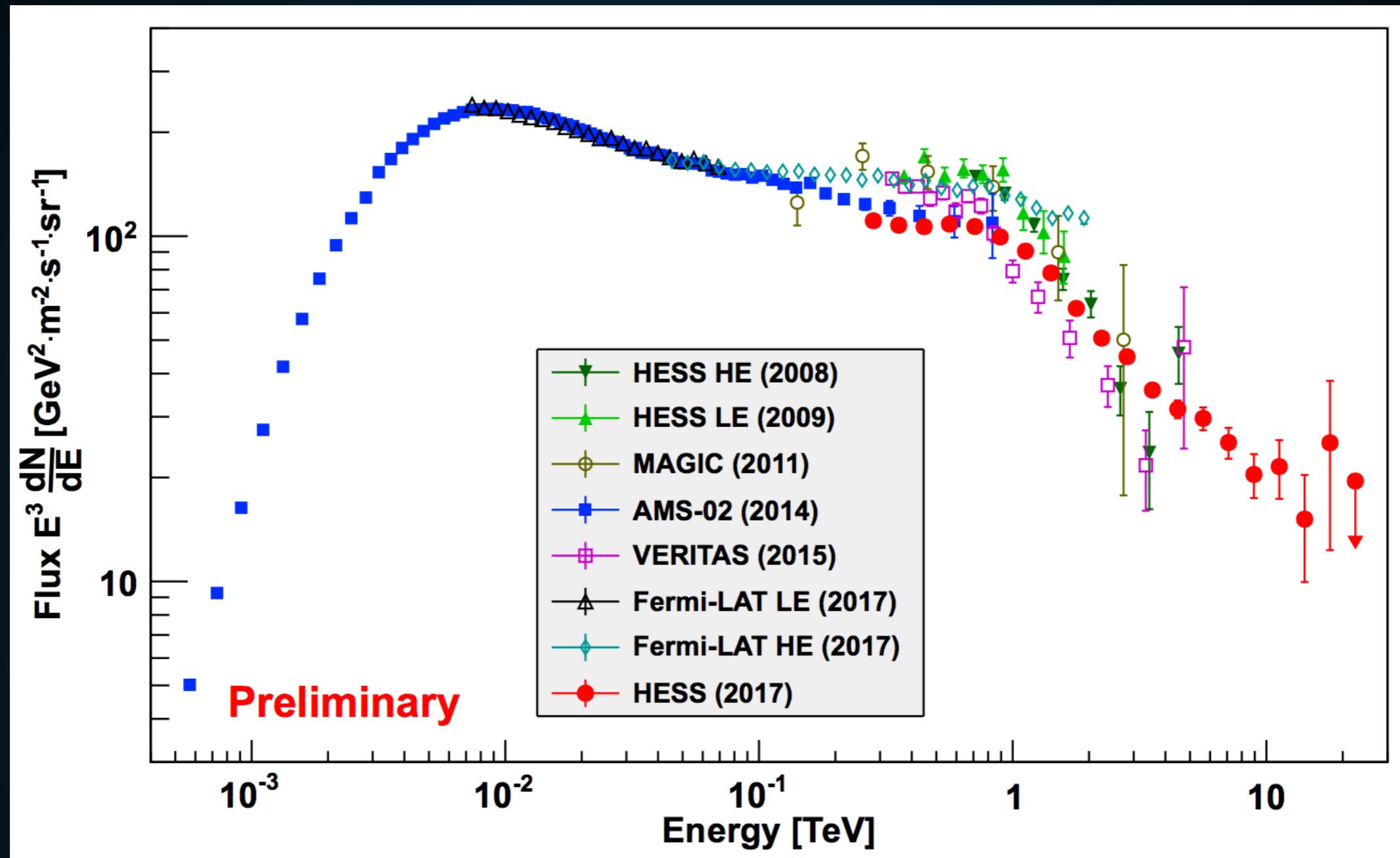
WHAT HAPPENS TO THE LOW-ENERGY e^+e^- ?

Ignore theoretical predictions:

Let TeV observations be your guide

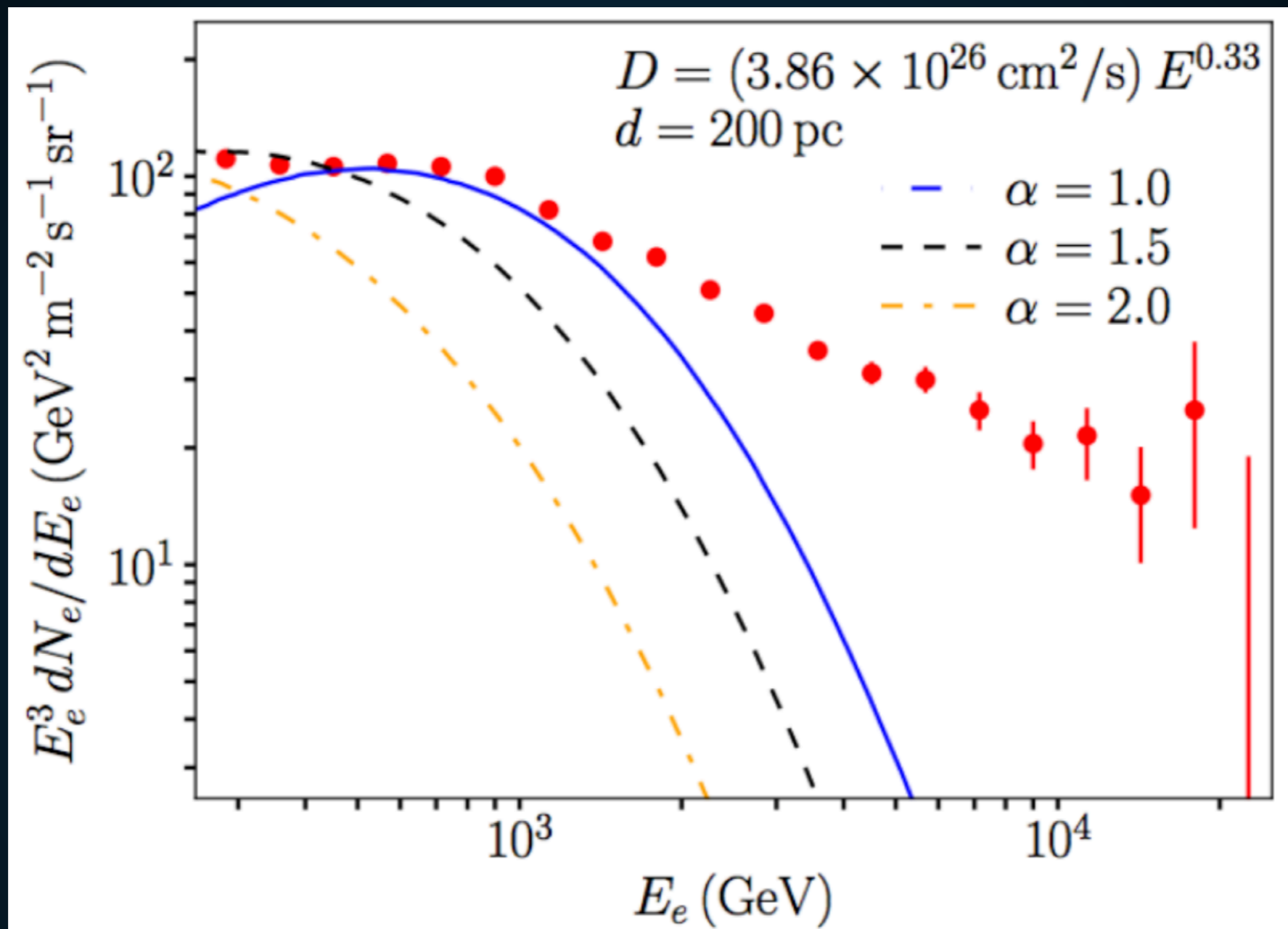


WHAT HAPPENS TO THE LOW-ENERGY e^+e^- ?



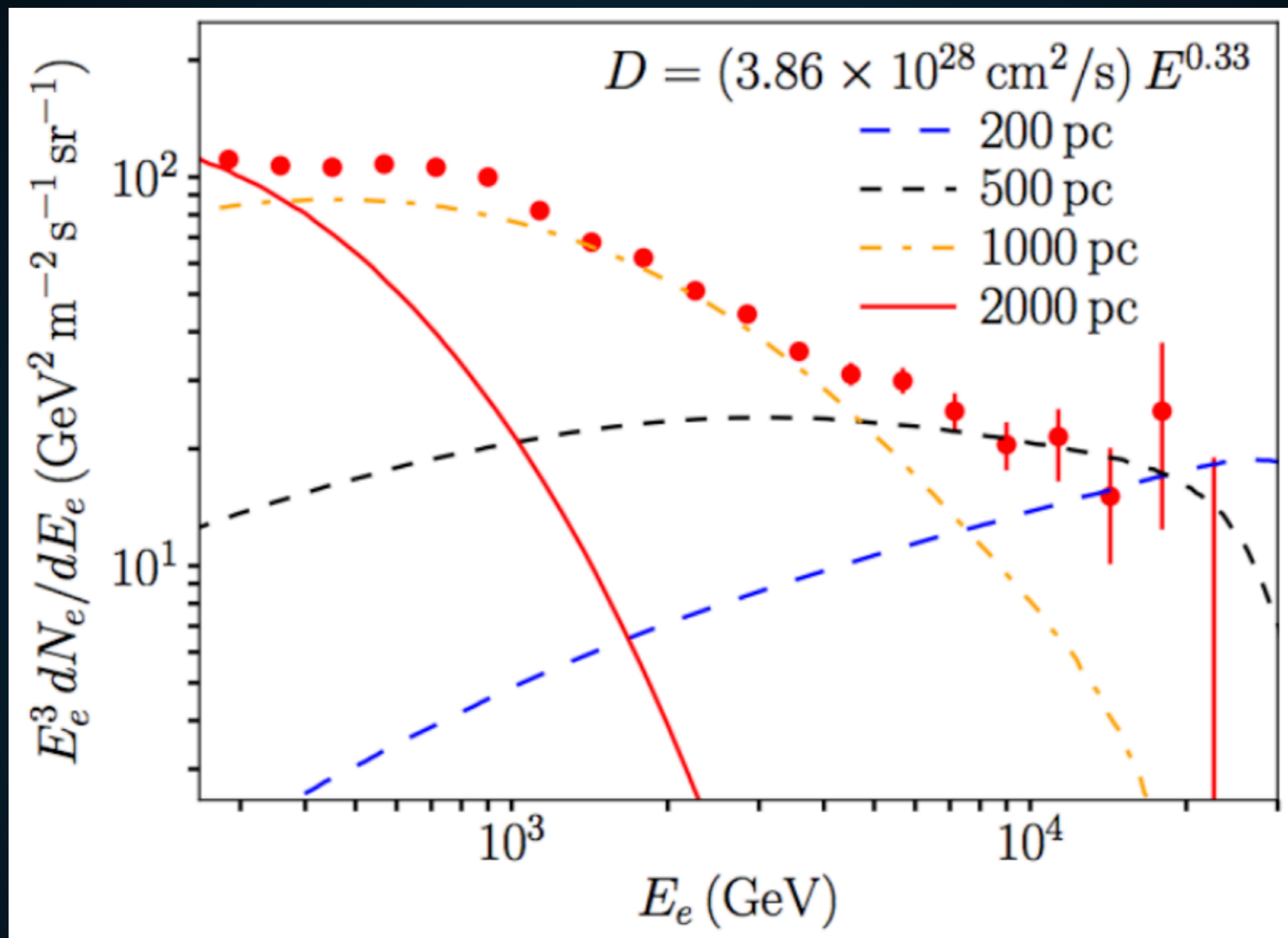
- ▶ Recent H.E.S.S. observations have extended the observed e^+e^- spectrum to energies exceeding 20 TeV.

WHAT HAPPENS TO THE LOW-ENERGY E^+E^- ?



- ▶ **Assumption 1:** If diffusion constant near Earth is low, any source explaining the electron flux must be within $\sim 30 \text{ pc}$ of Earth.

WHAT HAPPENS TO THE LOW-ENERGY E^+E^- ?



- ▶ **Assumption 2:** If diffusion is high, the nearest 10 TeV source can be ~ 500 pc away.

WHAT HAPPENS TO THE LOW-ENERGY e^+e^- ?

- ▶ There are no high-energy sources within 30 pc sources.
- ▶ Gamma-Ray Observations rule out any such source.
- ▶ Thus, diffusion near Earth is high.

- ▶ What were the uncertainties in pulsar models?

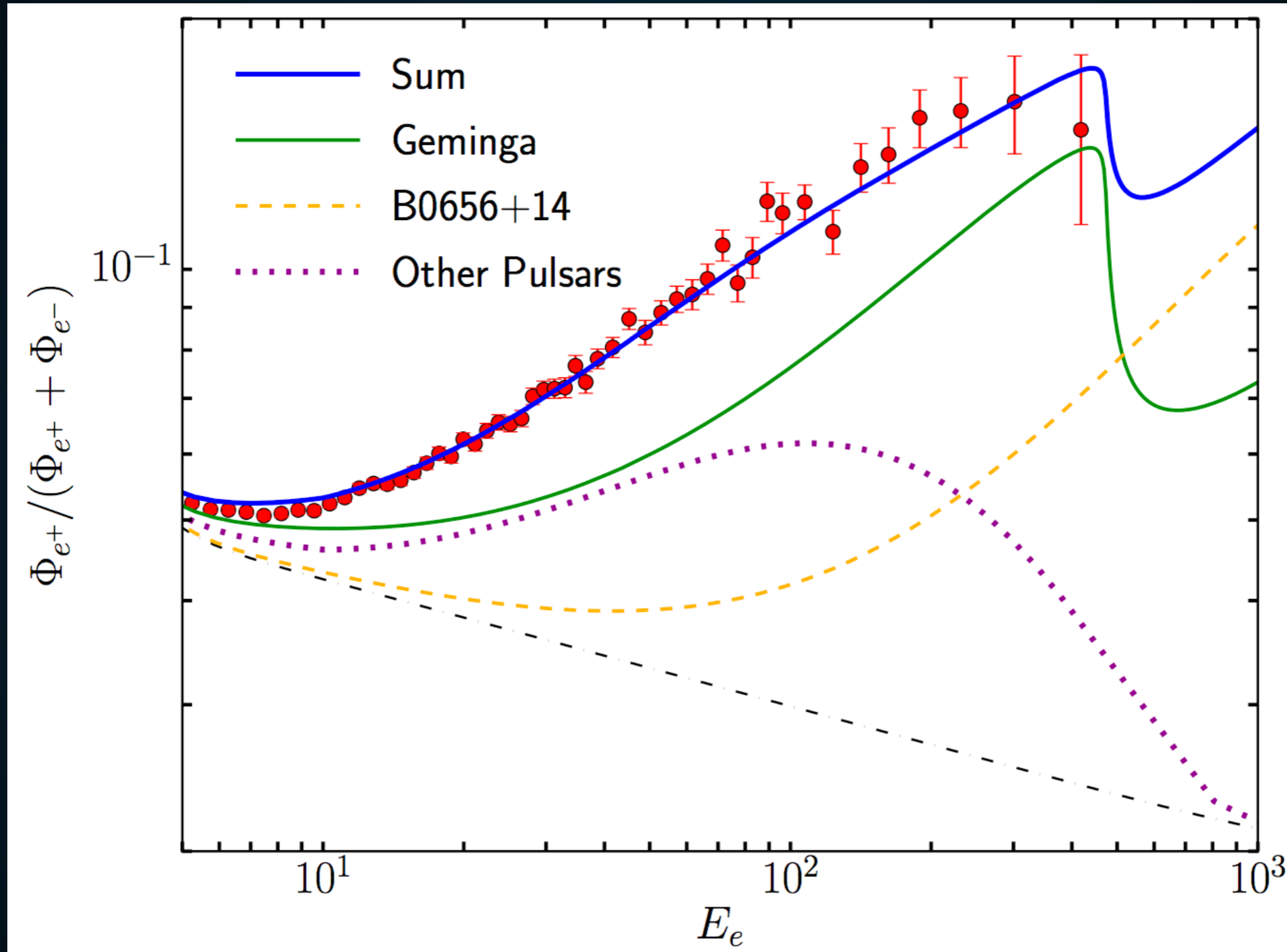
- ▶ I: The e^+e^- production efficiency?

- ▶ II: The e^+e^- spectrum.

- ▶ III: The propagation of e^+e^- to Earth. [Malyshev et al. \(0903.1310\)](#)

- ▶ The observed spectrum on Earth of electrons and positrons injected by pulsars is also strongly dependent on propagation effects. In particular, the observed cutoff in the flux of electrons from a pulsar can be much smaller than the injection cutoff due to energy losses (“cooling”) during propagation. We define the cooling break, $E_{br}(t)$, as the maximal energy electrons can have after propagating for time t . Since – as stated above – the typical

THE POSITRON FRACTION FROM TEV HALOS

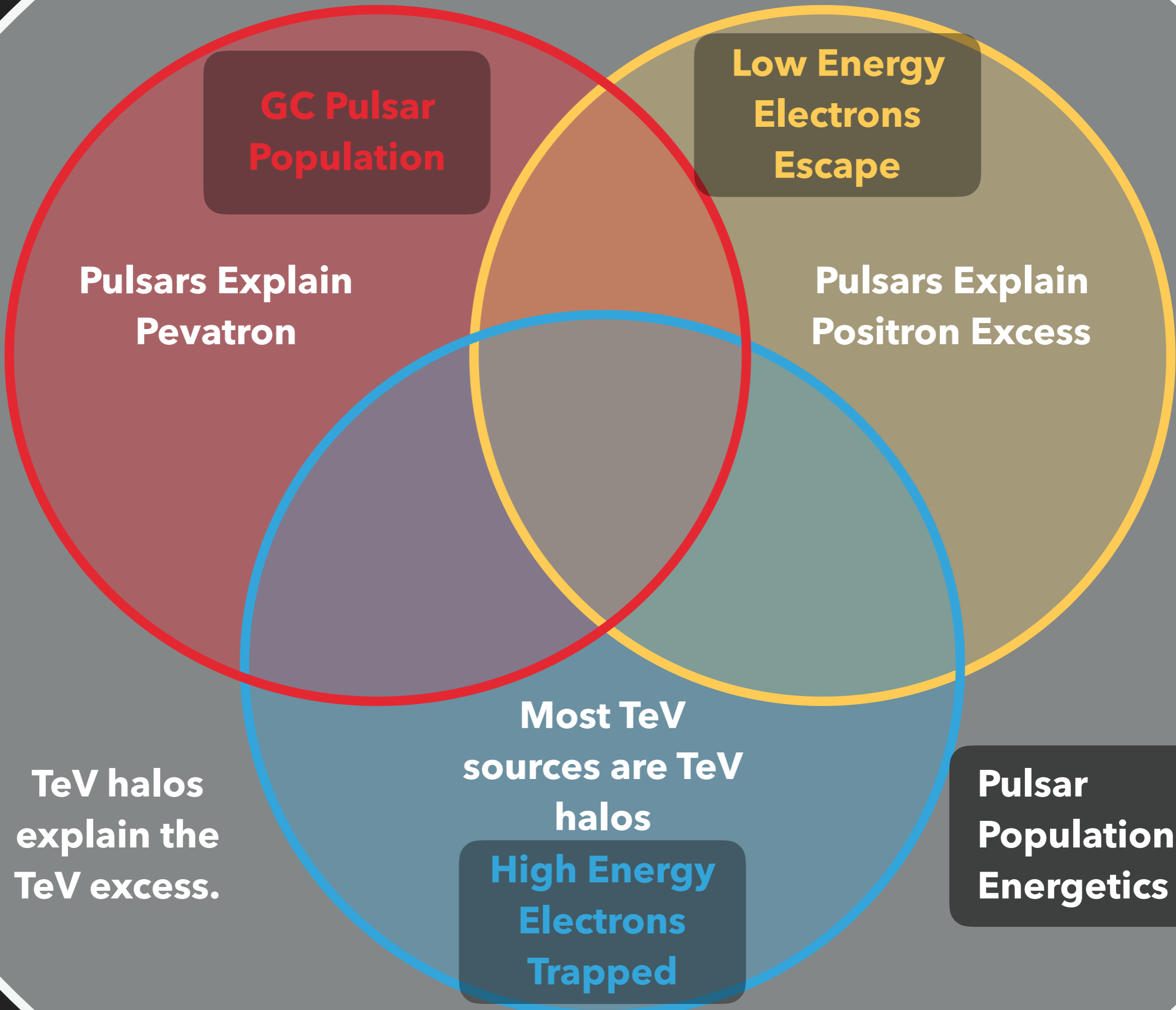


- ▶ Reasonable models can be exactly fit to the excess.

CONCLUSIONS (1/2)

- ▶ **TeV observations open up a new window into understanding cosmic-ray propagation.**
- ▶ **TeV observations from HAWC and HESS have answered all three uncertainties regarding pulsar positron production.**
 - ▶ **Pulsars efficiently convert their spindown power to e^+e^-**
 - ▶ **These e^+e^- are injected with a hard spectrum.**
 - ▶ **These e^+e^- propagate efficiently to Earth.**
- ▶ **This provides extremely strong evidence for the pulsar interpretation.**

- ▶ **TeV Halo observations have much more to teach us:**
 - ▶ **TeV halos are a new tool for finding pulsars that are not beamed towards Earth (TL et al. 1703.09704)**
 - ▶ **TeV halos produce the vast majority of unassociated TeV sources (TL et al. 1703.09704)**
 - ▶ **TeV halos produce the diffuse Milagro TeV excess (TL & Buckman 1707.01905)**
 - ▶ **TeV halos produce the Galactic Center Pevatron (Hooper, Cholis, & TL 1705.09293)**



GC Pulsar Population

Low Energy Electrons Escape

Pulsars Explain Pevatron

Pulsars Explain Positron Excess

TeV halos explain the TeV excess.

Most TeV sources are TeV halos

Pulsar Population & Energetics

High Energy Electrons Trapped